NEW MATERIALS AND PROCESSES

Advanced Industrial Materials (AIM) Fellowship Program

Deborah Duncan McCleary
Science and Engineering Education
Oak Ridge Institute for Science and Education
Oak Ridge, Tennessee 37830

Peter Angelini
Metals and Ceramics Division
Oak Ridge National Laboratory
P. O. Box 2008, Oak Ridge, Tennessee 37831

INTRODUCTION

The Advanced Industrial Materials (AIM) Program administers a Graduate Fellowship Program focused toward helping students who are currently under-represented in the nation's pool of scientists and engineers to enter and complete advanced degree programs. The objectives of the program are to (1) establish and maintain cooperative linkages between the Department of Energy (DOE) and professors at universities with graduate programs leading toward degrees or with degree options in Materials Science, Materials Engineering, Metallurgical Engineering, and Ceramic Engineering, the disciplines most closely related to the AIM Program at Oak Ridge National Laboratory (ORNL); (2) strengthen the capabilities and increase the level of participation of currently underrepresented groups in master's degree programs; and (3) offer graduate students an opportunity for practical research experience related to their thesis topic through the 3-month research assignment or practicum at ORNL.

There were two participants in the fellowship program for FY 1998: Aszetta Jordan, University of Cincinnati, and Michelle Lian, Virginia Polytechnic Institute and State University. The program is administered by the Oak Ridge Institute for Science and Education (ORISE). Ms. Lian completed all requirements in August 1998. Ms. Jordan was extended one quarter and is expected to complete requirements in March 1999.

One new student, Sherman McElroy, was appointed in August 1998. He is a graduate student at the University of Alabama in the Metallurgical and Materials Science Engineering Department. His research advisor is Dr. Ramana Reddy. The name of their project is Laser Surface Treatment of Cast Aluminum Alloy Automobile Cylinder Blocks for Wear Resistance. McElroy will be conducting casting experiments and sample characterization studies at ORNL.

The abstracts on the following pages summarize the activities of the Jordan and Lian.

Advanced Industrial Materials (AIM) Fellowship Program

Section 1. The Influence of Minor Alloying Additions on Material Behavior in FeAl and Ni_3Al-Based Intermetallics

A. Jordan and O. N. C. Uwakweh
Materials Science and Engineering Department
University of Cincinnati
498 Rhodes Hall, Cincinnati, Ohio 45221-0012

P. J. Maziasz
Metals and Ceramics Division
Oak Ridge National Laboratory
P.O. Box 2008, Oak Ridge, Tennessee 37831

INTRODUCTION

This study was a joint project with Oak Ridge National Laboratory (ORNL) to evaluate the effects of minor elemental additions on the microstructure and phase transformations of iron- and nickel-based aluminides. These materials have great potential for use in structural applications because they have an excellent combination of high-strength, corrosion, and oxidation-resistance properties. However, a major concern is that these materials possess low ductility and poor resistance to fracture in room-temperature environments. In addition, these alloys are susceptible to solidification cracking, which in turn affects their ability to be welded. While an extensive amount of work has been geared towards improving the ductility and resistance to brittle fracture in these materials, little information exists concerning their solidification behaviors and pertinent phase transformations resulting from the addition of minor elements. Knowledge of the phase-transformation kinetics occurring during the heating and cooling of these materials (i.e., simulated welding process) is essential to tailoring a specific welding technique for creating sound, defect-free welds. The focus of this study is to evaluate the phase-transformation sequence of the alloys in their pre-existing condition, for the purpose of understanding and predicting the behavior of these materials during certain process applications such as welding.

TECHNICAL PROGRESS: FY 1998

Overview of Results

Based on the experimental results, the role of minor elemental additions in the materials has been determined. The distinctions resulting from the minor elemental additions are observed in the microstructures of the as-cast materials. The microstructures showed that the addition of Mo and B to the binary FeAl material (i.e., simpler alloys containing Fe-Al-Mo and Fe-Al-Mo-B) produced grain structures that were nondendritic in nature, whereas the additions of Zr and C (i.e., complex alloys containing Fe-Al-Mo-Zr-C and Fe-Al-Mo-Zr-C-B) revealed dendritic-type structures. The distinctions in the

microstructural features also have an impact on the transformation behavior in these materials as revealed through differential scanning calorimetry (DSC), X-ray diffraction (XRD), and Mössbauer measurements.

From the DSC results, we observed a distinct invariant reaction peak above 1250ºC in the heating and cooling curves. The invariant reaction was detected only in the dendritic-type material structures. In the XRD patterns, the dendritic-type materials (i.e., Fe-Al-Mo-Zr-C and Fe-Al-Mo-Zr-C-B) revealed an $AlFe_3C_{0.5}$ phase that was not detected in the nondendritic-type microstructures. From Mössbauer effect measurements, the peak at –0.9 mm/s, which is present in the simpler alloys, is not discernable in the complex or dendritic materials. This suggests that the local Fe environment is highly influenced by the presence of Zr and C in the base binary, ternary, and quarternary alloys. Since all of the FeAl-based materials were prepared through a casting operation, the results in this study suggest that the addition of Zr and C affected the solidification rates, thus leading to the development of the dendritic microstructure.

The overall observations made between the simpler and complex materials also have a direct affect on the material behavior. This was confirmed through microhardness and weld-simulation testing. For instance, microhardness testing revealed that the dendritic-type microstructures yield higher hardness values than those nondendritic microstructures. And finally, weld simulations showed that the propagation of cracks was eliminated in the materials with dendritic-type growths in the microstructures.

TECHNICAL RESULTS

The binary FeAl and Ni_3Al materials have primary physical and mechanical properties that can be enhanced significantly through minor alloying. Although significant progress has been made in efforts to commercialize the FeAl and Ni_3Al alloys, important issues related to their processing and weldability, for example, have not been resolved completely. In this study, a systematic approach was taken to better understand the influence of minor elemental additions (i.e., Mo, Zr, and B) on the microstructure, thermal stability, and the potential weldabilities of the FeAl- and Ni_3Al-based materials.

A series of FeAl- and Ni_3Al-based materials was prepared by arc melting and then drop-cast into copper chill molds. DSC measurements from ambient to 1500°C were used to identify transition temperatures associated with their thermal evolution characteristics by employing continuous heating and cooling cycles. The as-cast materials were further characterized using such techniques as optical microscopy, XRD, Gleeble simulation, and ^{57}Co Mössbauer effect measurements on selected materials with iron as a constituent.

DSC results for both the FeAl- and Ni_3Al-based materials showed distinct metastable transitions that occurred below 850°C during heating for varied scan rates but were irreversible upon cooling. In addition, melting, solidification, and invariant reactions associated with their structural changes were observed at higher temperatures. Based on DSC results, it is evident that certain characteristic peaks associated with the metastable transition processes are diffusion controlled or thermally activated. The activation energies for these processes were determined based on non-isothermal kinetics studies. It

was found that metastable transitions observed below 850°C were associated with artifacts introduced during sample preparation prior to DSC measurements.

Optical microscopy of the as-cast materials revealed distinct microstructures, where the FeAl materials, in particular, can be discussed under two different categories. The binary FeAl, ternary Fe-Al-Mo, and quaternary Fe-Al-Mo-B materials revealed varying grain sizes averaging between 195 and 272 µm The FeAl-based materials containing Zr and C additions (i.e., Fe-Al-Mo-Zr-C and Fe-Al-Mo-ZrC-B) revealed dendritic growths in their microstructures. All of the Ni_3Al-based materials showed the existence of dendritic-type growths in the microstructure.

Initial XRD patterns of the FeAl- and Ni_3Al-based materials were used to identify the phases present in their as-cast conditions. The structural evolutions discerned with heat treatments were corroborated with X-ray diffraction and Mössbauer effect studies in the as-cast and aged states of the FeAl-based materials.

Gleeble simulation studies of the weldability of these materials suggest that for the FeAl-based materials additions of B, Zr, and C are beneficial (individually or in combination) to crack resistance following weld thermal cycles. However, in the Ni_3Al-based materials evaluated, results suggest that for an optimum level of Zr *(i.e., Zr levels within 1.7 to 3.0 wt %),* intergrannular cracking is prevented.

In the DSC measurements, we note the different exothermic and endothermic peak profiles and their subsequent relation with structural evolution. From the heating and cooling curves, one can affirm the presence of low-temperature (i.e., less than 765°C) metastable transitions, (which are irreversible upon cooling), as well as indications of the formation of the Ni-Ni_5Zr eutectic reaction in the materials studied. These solid-state reactions are metastable transitions like those observed at low temperatures in the FeAl materials, and they can be eliminated by using solid samples as opposed to filings from the bulk material. While optical microscopy examinations revealed dendritic structures, SEM confirmed the existence of the Ni-Ni_5Zr eutectic.

The welding behavior of the Ni-Al-Cr-ZrB (1.7 wt % Zr) material shows strong resistance to cracking, whereas both the Ni-Al-Cr-Zr-B (3.0 wt % Zr) and Ni-Al-Cr-Zr-Mo-B materials showed excessive cracking. In comparing the two Ni-Al-Cr-Zr-B materials, it is obvious that there must be an optimum level of the Zr (i.e., 1.7 wt %), whereby increasing its amount (i.e., 3.0 wt %) would result in increased cracking severity.

CONCLUSIONS

A comprehensive experimental study was conducted on the FeAl and Ni_3Al-based alloys in order to evaluate the influence of minor elements of addition with respect to material microstructure, welding behavior, and thermal stability. Based on the results, the following conclusions can be drawn:

FeAl Materials

1. The as-cast microstructures of the FeAl-based materials were found to differ. A nondendritic grain structure was found to develop in the FeAl, Fe-Al-Mo, and Fe-Al-Mo-B materials, with grains averaging 244, 195, and 272 µm, respectively. On the other hand, additions of Zr and C produced dendritic-type microstructures in the complex Fe-Al-Mo-Zr-C and Fe-Al-Mo-Zr-C-B materials.

2. The differences in microstructures were corroborated through thermal analysis and XRD measurements. Based on DSC measurements, the materials all transformed through a metastable transition below 859ºC, which was determined to be associated with artifacts introduced during sample preparation (filing). Additional thermal-analysis studies revealed that the metastable transition in these materials could be avoided by using solid specimens in lieu of powders obtained from filings. For temperatures above 850ºC, distinctions were made between the simpler and complex alloys. This was realized through the invariant reactions observed at 1281 to 1289ºC and 1254 to 1280ºC, respectively, during heating and cooling of the complex Fe-Al-Mo-Zr-C-B materials. In retrospect, this was not observed in the simpler FeAl, Fe-Al-Mo, and Fe-Al-Mo-B materials. From the perspective of XRD measurements, peaks corresponding to an $AlFe_3C_{0.5}$ phase were observed in both the Fe-Al-Mo-Zr-C and Fe-Al-Mo-Zr-B materials but were absent in the FeAl, Fe-Al-Mo, and Fe-Al-Mo-B materials.

3. The application of non-isothermal kinetic analysis as applied to the metastable transitions observed in the DSC measurements below 850°C reveal the occurrence of diffusion-controlled processes. The diffusion-controlled or thermally induced process occurred in the FeAl, Fe-Al-Mo, and Fe-Al-Mo-Zr-C materials, with activation energies determined to be 721, 89, and 101 kJ/mole, respectively.

4. The addition of Mo (Fe-Al-Mo) caused considerable microstructural changes in its as-cast and aged states. The addition of Mo produced an equiaxed microstructure prior to aging. However, after aging at 740°C for 1 h, columnar (elongated) grains were observed to appear along a preferred orientation. Although pole-figure measurements showed some texturing effects in the as-cast material, no texture orientation was found to develop after subsequent aging. This, in turn, eliminates the possibility that the unusual microstructure resulting from aging is associated with texturing effects.

5. Mössbauer-effect measurements show similar Fe environments in the as-cast state for all of the materials studied. An Fe environment with a large QS of 1.680 mm/s was observed in the Fe-Al-Mo material after aging at 740°C for 1 h. This shows the existence of a critical stage of structural change in this material (i.e., reshuffling of atomic species over large distances). Results further show that aging of the binary FeAl at 739°C for 1 h and the Fe-Al-Mo-B at 746°C for 1 h did not lead to the establishment of a fully ordered (i.e., equilibrium) material.

6. Finally, results show that the most promising FeAl-based materials for welding purposes appear to be Fe-Al-Mo-B, Fe-Al-Mo-Zr-C, and Fe-Al-Mo-Zr-C-B (depending on the intended application). This is because the additional elements of B, Zr, and C tend to mitigate crack propagation when welding temperatures approach 1200°C. Because hardness values correlate the tensile strength of these materials, the Fe-Al-Mo-Zr-C–type alloy would be best utilized for applications requiring high-strength properties with the ability to maintain structurally sound welds.

Ni_3Al Materials

1. Metallographic analysis of the Ni-Al-Cr-Zr-B (1.7 wt % Zr), Ni-Al-Cr-Zr-B (3.0 wt % Zr) and Ni-Al-Cr-Zr-B-Mo-B materials all showed dendritic type microstructures.

2. DSC measurements at various scan rates, for the Ni-Al-Cr-Zr-B (1.7 wt % Zr), Ni-Al-Cr-Zr-B (3.0 wt % Zr), and Ni-Al-Cr-Zr-B-Mo-B materials, revealed the presence of a peak that is associated with the Ni-Ni_5Zr eutectic as noted in the Ni-Zr phase diagram at 1170°C.

3. SEM analysis of the Ni-Al-Cr-Zr-B (1.7 wt % Zr) alloy confirmed the existence of the Ni-Ni_5Zr eutectic microconstituent.

4. Based on Gleeble simulations, the welding behavior of these materials, when reaching a peak temperature of 1194°C, showed that two of the three alloy compositions were susceptible to intergrannular cracking. The experimental results show that cracking is prevalent in the Ni-Al-Cr-Zr-B (3.0 wt % Zr) and Ni-Al-Cr-Zr-B materials, whereas no cracks are observed in Ni-Al-Cr-Zr-B (1.7 wt % Zr). The results suggest that cracking is influenced by the amount of Zr concentrations and also by elemental additions of Mo.

SUGGESTIONS FOR FUTURE WORK

Future work in this research area could be pursued in the following manner:

Transmission electron studies of the as-cast and aged materials would be beneficial in showing their dislocation structures. These images would be especially useful in the ternary Fe-Al-Mo material, which revealed variances in the hardness values when aged and quenched from different temperatures.

In the author's opinion, it also would be interesting to determine the optimum level of Zr in the Ni-Al-Cr-Zr-B materials by allowing the amount to vary between 1.7 and 3.0 wt % in order to establish their resistance to weld cracking.

PUBLICATIONS

A. Jordan and O. N. C. Uwakweh, "The study of Mechanically Alloyed Fe-Zn-Si Intermetallic Phases," accepted for publication in the *Journal of Materials Synthesis and Processing* (February 1997).

Jordan and O. N. C. Uwakweh "Verification of Sandelin Phenomenal in Mechanical Alloyed Fe-Zn and Fe-Zn-Si," accepted for publication in *Materials Transactions, JIM* (November 1997), scheduled to appear in Vol. 38, No. 12.

O. Uwakweh and A. Jordan, "Application of Metastable Transformation of Mechanically Alloyed Fe-Zn-Si in Equilibrium Phase Studies," *Journal of Phase Equilibria*, Vol. 18, No. 5, pp. 448–57, (1997).

O. N. C. Uwakweh, Z. Liu, A. Jordan, B. Chakoumakos, S. Spooner, and P. Maziasz, "Neutron Diffraction and Phase Evolution of the Mechanically Alloyed Intermetallic Compound ζ-$FeZn_{13}$," accepted for publication in *Metallurgical and Materials Transactions* (July 1997).

O. Uwakweh, A. Jordan, and P. Maziasz, "Thermal Transformations in Mechanically Alloyed Fe-Zn-Si Materials," accepted for publication in *Metallurgical and Materials Transactions* (May 1997).

A. Jordan and O. N. C. Uwakweh, "Structural Evolution and Kinetics Studies of Mixed Phases Terminal Solid Solutions of Fe-Zn and Fe-Zn-Si Alloys," submitted to the *Journal of Materials Research* (October 1997).

A. Jordan, Z. Liu, and O.N.C. Uwakweh, "Mechanical Alloying Studies in the $\Gamma(Fe_3Zn_{10})$ and $\Gamma_1(Fe_5Zn_{21})$ Single and Mixed Phase Compositions," submitted to the *Journal of Materials Research* (April 1997).

A. D. Jordan, "The Influence of Minor Alloying Additions on Material Behavior in FeAl- and Ni_3Al-based Intermetallics," Ph.D. dissertation submitted to the Division of Research and Advanced Studies of the University of Cincinnati, 1999; committee professor, Professor Oswald N. C. Uwakweh.

POSTER SESSIONS

Jordan, "Phase Evolution in Mechanically Alloyed Fe-Zn-Si Ternary Alloys," presented at the annual meeting of the AIM program, sponsored by the Advanced Industrial Materials program, held in Albuquerque, New Mexico, on June 16–18, 1997.

HONORS AND AWARDS

A. D. Jordan, Advanced Industrial Materials Program Ph.D. Fellowship, administered by the Oak Ridge Institute for Science and Education (ORISE), 1996 to present.

Advanced Industrial Materils (AIM) Fellowship Program

Section 2. Mechanical Behavior of Epoxy-Bonded Steel for Leaking Pipe Repair

Michelle K. Lian
Department of Materials Science and Engineering
Virginia Polytechnic Institute and State University
Blacksburg, Virginia 24061

Jim R. Keiser and Dane F. Wilson
Corrosion Science and Technology Group
Metals and Ceramics Division
Oak Ridge National Laboratory
P.O. 2008, Oak Ridge, Tennessee 37831

OBJECTIVE

There are instances where efficiency and safety may be compromised as a result of leaking pipes. Consequently, it is sometimes necessary to shut down the entire operation to fix the leak. Thus, it is worth evaluating other repair methods that can patch the leak for a temporary period without shutting down the operation while a new pipe is being constructed. The objective of this project is to evaluate the mechanical properties of epoxy-bonded steel in the aqueous environments that might be the conditions of such repair.

MATERIALS

There were three components in the epoxy system: EPON® resin 828, dicyandiamide, and 2-methylimidazole. N, N-dimethyl formamide was used to dissolve dicyandiamide. Steel was chosen as the substrate.

SAMPLE PREPARATION

The neat epoxy bars were cast in a silicone mold. The epoxy resin was composed of EPON® resin 828, dicyanidiamide (4 wt % of EPON® 828), and 2-methylimidazole (0.5 wt % of EPON® 828). Dicyandiamide was used as the curing agent, and 2-methylimidazole was used as the catalyst. Dicyandiamide and 2-methylimidazole were dissolved in N, N-Dimethyl formamide before the addition of EPON® 828. The resin system was poured into the silicone mold, and it was placed in an oven at 50°C overnight to evaporate the solvent. The oven temperature was then increased gradually to 180°C, and the resin system was cured for an hour at 180°C. The oven was allowed to cool down slowly to avoid thermal shock of the samples.

The steel surface was prepared using one of the following methods: scrubbing with soap and water, sanding with 220-grit sandpaper, or sandblasting. The surface-treated steel

bars were sealed to the silicone mold using a silicone sealant. The epoxy resin was prepared and poured into the cutouts of the silicone mold. The curing schedule of the neat epoxy bars was followed, and this created epoxy-bonded samples.

EXPERIMENTS

The testing program consisted of four sample types: neat epoxy bars and an epoxy-bonded steel with three different surface treatments. Four to five samples from each type were exposed in air before the mechanical testing. The rest of the samples were divided into 16 groups of 4 to 5 each for exposure in 2 aqueous environments for 2 time periods. Each sample group was placed in separate plastic bottles filled with solution, and they were positioned in a distilled-water bath at 50°C. Two aqueous solutions were used in the plastic bottles: distilled water and a 3.4% NaCl solution in distilled water. The samples were exposed for periods of 1 or 2 weeks.

The initial and final weights of the epoxy bars were measured to determine the moisture uptake of the epoxy bars in the aqueous environments. The three-point bend test was used to evaluate the mechanical properties of the neat epoxy bars and the epoxy-bonded samples. The testing was performed using the Universal Testing Machine L-200 at room temperature. The cross-head speed was set at 2.5 mm/min. The span length was 20 mm for epoxy bars and 90 mm for epoxy-bonded steel.

Scanning electron microscopy (SEM) was used to study the fracture surfaces to determine the location of failure. Optical microscopy also was used to help study the fracture surfaces.

RESULTS

The average weight gain for the epoxy bars was 3.96% in distilled water and 3.21% in NaCl solution after 1 week and 8.51% and 8.70% in distilled water and in NaCl solution, respectively, after 2 weeks. The Young's modulus of the epoxy bars was calculated using the following equation:

$$E = \frac{F \cdot L^3}{4 \cdot \delta \cdot w \cdot d^3}$$

where

E = Young's modulus of the epoxy bar

F = loading force

L = length of the epoxy bar

δ = deflection of the epoxy bar

w = width of the epoxy bar

d = thickness of the epoxy bar

A student's T test was used to test the independence of each data group. The two data groups that have higher probability to be independent of each other are likely to yield lower value from the Student's T test. This means that the two data groups are statistically different from each other.

The steel was analyzed for its chemical content. The bonded samples failed when the epoxy was popped off the steel substrate by shear force. Thus, the fracture surface studied was the bonded surface of the steel or the epoxy. The fracture surfaces of the failed samples were studied to determine the failure location. It was observed by visual inspection that oxide was present on the epoxy surface. Using the optical microscope in the transmission mode, oxide was seen on the epoxy surface. SEM study of the steel substrate showed that no epoxy was present on the steel surface.

CONCLUSIONS

The average shear stress and the average axial stress of the epoxy-bonded samples decayed with time for all three surface treatments in both aqueous environments. The solution, distilled water or 3.4% NaCl solution, had penetrated and weakened the interface. Therefore, the bond strength decreased with increasing exposure time.

Advanced Materials for High-Temperature Liquid-Metal Corrosion and Erosion Resistance

M. Trkula, M. A. Nastasi, K. C. Walter, and K. V. Salazar
Materials Science and Technology Division
P.O. Box 1663, MS-E549
Los Alamos National Laboratory
Los Alamos, New Mexico 87545

INTRODUCTION

Die life is a major consideration in the die-casting process; in many cases a complicated die may cost more than the die-casting machine itself. The die lifetime can vary from 20,000 to more than 250,000 parts, depending on the die material, die design, material being cast, and the thermochemical processes involved. During the die's service life, die inserts and cores experience a large number of thermomechanical cycles, which thermally fatigue the die and result in the development of a network of fine cracks in the die surface (i.e., heat checking). In addition to heat checking, other such wear and failure modes as erosive and abrasive wear, chemical attack and/or corrosion, and soldering between the die and casting material are life-limiting factors for die-casting dies.

Aluminum is an important and energy-strategic material in U.S. industry for which die casting is a principal manufacturing method. Aluminum is a material of choice when a high strength-to-weight ratio is required in structural components, and it is used widely in the automotive and aerospace industries.

The increased demand for cast aluminum parts in U.S. industry has led to the development of casting machines that use ever higher injection speeds and higher casting pressures. However, the result of operating the dies at such extreme conditions is excessive die wear due to erosion, thermal fatigue, and surface reactions. These wear mechanisms result in die life that is, in many instances, less than desirable. After production of as few as 40,000 parts, a die may require complete refurbishing. Industry estimates that 30 to 40% of die-casting machine downtime results from die wear. This means lost productivity and represents a significant opportunity for process improvement and cost reduction.

In response to this problem, we are developing a cost-effective and industrially relevant surface-engineering process involving the combination of materials science, plasma-immersion processing, and organometallic chemical vapor deposition (CVD) techniques. This non-line-of-sight process allows easy processing of complex shapes and also is inherently scaleable to allow for the processing of extremely large components. The immediate objective is to develop corrosion- and erosion-resistant, thermodynamically stable, and highly adherent conformal coatings on die materials used to cast aluminum and other metals.

TECHNICAL APPROACH

Candidate corrosion- and erosion-resistant coatings are chosen based on an analysis of thermodynamic and thermal expansion for the total system of liquid metal/coating/substrate. Coating synthesis will employ a combination approach using organometallic (OM) CVD with plasma-immersion ion processing (PIIP). The PIIP process will be used to physically and chemically clean the substrate surface, and to ion implant the coating species into the substrate surface to provide a graded transition to the coating. PIIP will be used in conjunction with OMCVD to deposit thick, adherent, and conformal surface coatings.

In PIIP, the item to be coated is immersed in a plasma. Ion implantation is used to increase coating adhesion and control coating stress. The combination of ion processing with deposition allows one to perform surface modification and produce graded materials and growth. In addition, the process produces coatings with superior adhesion with a thickness of tens of µm. The PIIP chamber (see Fig. 1) measures 1.2 by 1.8 m. The system is supplied with three rf supplies (two at 0.46 MHz, 3 kW, and one at 13.56 MHz, 1 kW), a 300-V 10-A dc supply, and two pulsed-voltage sources (10 kV, 10 kW, and 1 kV, 1 kW). Process-analysis instrumentation features a microwave interferometer, optical spectrometer, Langmuir probe, and residual gas analysis. Gases are supplied with precision mass-flow controllers, and the system is evacuated with a 1600-l/s turbomolecular pump.

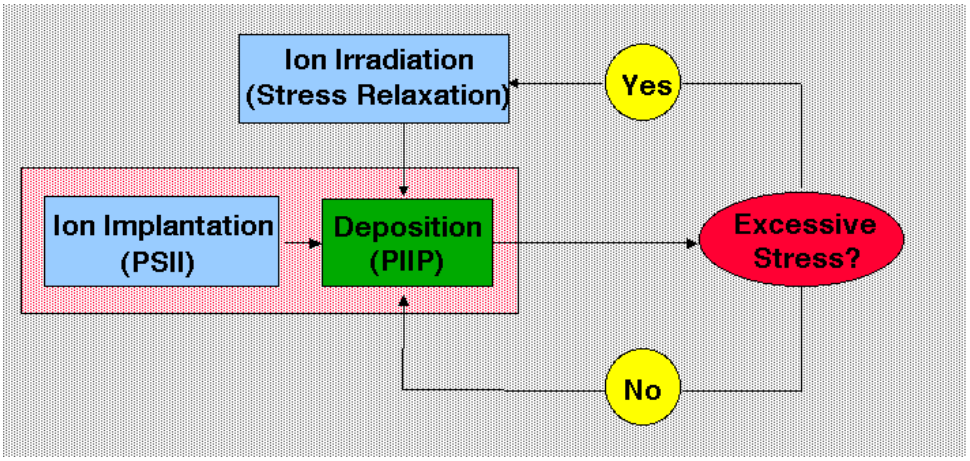

Fig. 1: An illustration of the process involved in the PIIP.

OMCVD is a process in which metal-organic or organometallic precursors are transported in the carrier gas to the reactor chamber. Here they decompose on a heated substrate and subsequently deposit a solid film, thereby resulting in elimination of volatile by-products. Inert carrier gases often are used to enhance the rate of transport of solid- or liquid-phase precursors to the reactor chamber. However, other reactive carrier gases also are used that participate in the chemistry of film deposition by acting as reducing or oxidizing agents. Epitaxial, polycrystalline, and amorphous films can be deposited, depending on the deposition conditions and the material to be deposited. The OMCVD process is illustrated in Fig. 2.

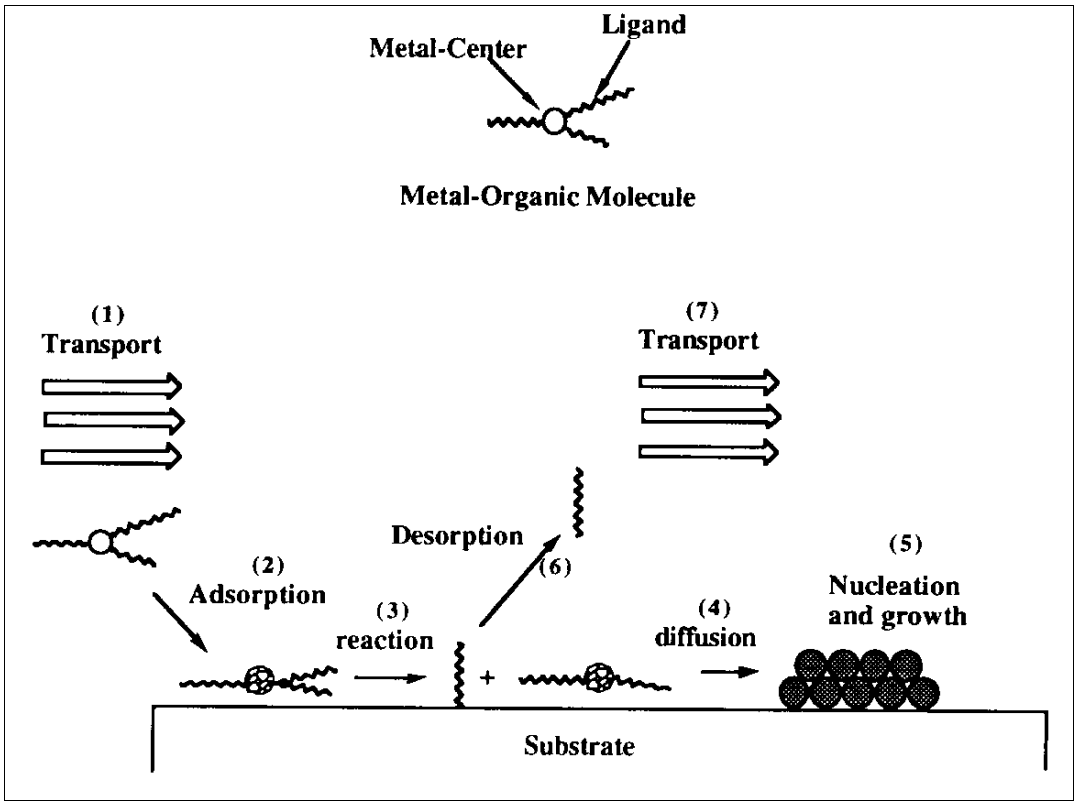

Fig. 2: An illustration of the process occurring in OMCVD.

TECHNICAL PROGRESS: FY 1998

Several coating materials have been developed during the past year. The PIIP process has been used to produce both B-C-H and Cr-C-O coatings. The B-C-H coatings were synthesized from various mixtures of diborane (B_2H_6) diluted with He and mixed with acetylene (C_2H_2). The synthesis was carried out at 20-mtorr pressure. The plasma was generated by the pulsed-glow discharge method with an applied voltage at 4 kV, which was pulsed at 4 kHz with a pulse width of 30 µs. The resulting deposition rate varied between 0.1 and 0.4 µm/h, depending on gas mixture. Typical coating hardness was in the 12- to 13-GPa range. X-ray diffraction showed the coating to be amorphous.

Coatings of Cr-C-O, which were deposited from $Cr(CO)_6$, possess a 1-torr vapor pressure at 36°C and decompose at 110°C. The $Cr(CO)_6$ was introduced into the processing chamber via a bubbler-heated set at 90°C without the use of carrier gas. The plasma was generated either by the application of 0.46-MHz capacitive rf source or by pulsed-glow discharge. The pressure during deposition was ~5 mtorr, and the deposition temperature varied between 20 and ~350°C. The deposition-applied voltage was 4 kV, which was applied at pulse frequencies between 4 and 20 kHz with a pulse width between 10 and 30 µs The resulting deposition rate varied between 0.15 and 10 µm/h, depending on plasma parameters and deposition temperature. Typical coating hardness was in the 14- to 20-GPa range, and X-ray diffraction showed the coating to be amorphous.

Wetting experiments were carried out by placing a high-purity Al sheet on the surface of coated and uncoated steel substrates. The samples then were placed in a high-vacuum furnace and heated to just above the Al melting temperature. The samples were held at temperature for 10 min before being cooled to room temperature. Figure 3 shows the results for both the B-C-H– and Cr-C-O–coated steel substrates and an uncoated 304 stainless steel substrate. These experiments show that Cr-C-O coatings provide effective protection against reactions between molten Al and steel substrates. The B-C-H coating was found to be not effective.

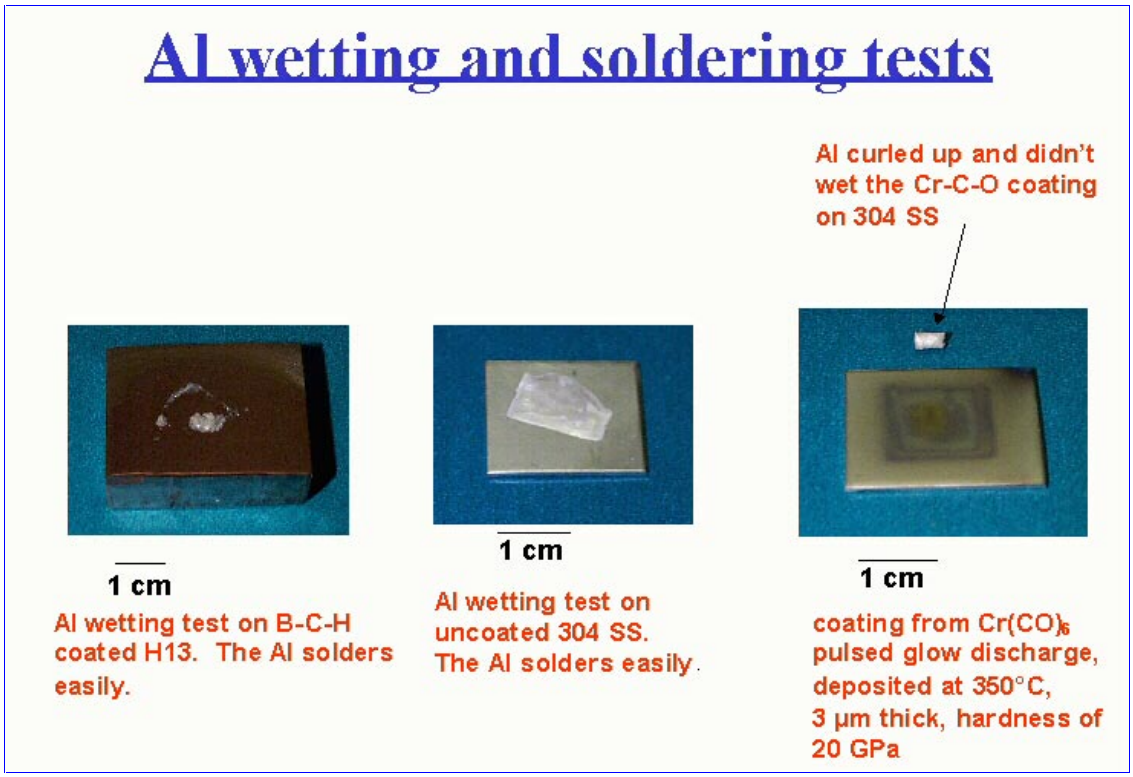

Fig. 3: Molten aluminum wetting test for B-C-H– and Cr-C-O–coated steel substrates and an uncoated 304 stainless steel substrate.

The OMCVD process was used to deposit both AlN and Er_2O_3 thin films. Aluminum nitride is a candidate material for protection against molten aluminum. We deposited aluminum nitride with OMCVD. The precursor gases were $Al[N(CH_3)_2]_3$ and NH_3. The homoleptic amide vapor was swept with helium gas. The deposition conditions were as follows: the NH_3 flow was fixed at 150 sccm, and the precursor reservoir was at 80°C. We varied the substrate temperature from 300 to 480°C; the pressure, between 1 and 10 torr; and the helium flow, from 150 to 450 sccm. Substrates were silicon and H-13 steel.

We determined the stoichiometry with RBS and the hydrogen content with ERD. The best films, where best is Al/N ratio ~ 1 and minimum hydrogen content, were obtained between 360 and 400°C, at 1 torr, with a helium flow of 150 sccm. These films were stoichiometric AlN with ~10% hydrogen content. Lower temperatures gave a

carbonitride, and higher temperatures gave an oxynitride. Deposition rates were 0.7 to 2.0 µm/min. Experiments with deuterated ammonia indicate that 90 to 95% of the hydrogen comes from the amide groupings on the precursor. We feel we have reduced the hydrogen content low enough to begin molten-metal testing.

Some literature reports cite erbium oxide as a protective material for molten iron. We deposited erbium oxide with OMCVD from $Er(tmhd)_3$ and O_2. The deposition conditions were 450°C and 10 torr. Our initial study concerned itself with deposition on stainless steel and H-13 tool steel. Figure 4 shows the two SEM micrographs of the deposited materials. Both materials show a fine grain structure and are stoichiometric. The material on H-13 shows some voids, and this probably results from corrosion of the H-13 in the O_2 environment. The Er_2O_3 on H-13 probably will require surface modification with PIIP before Er_2O_3 OMCVD.

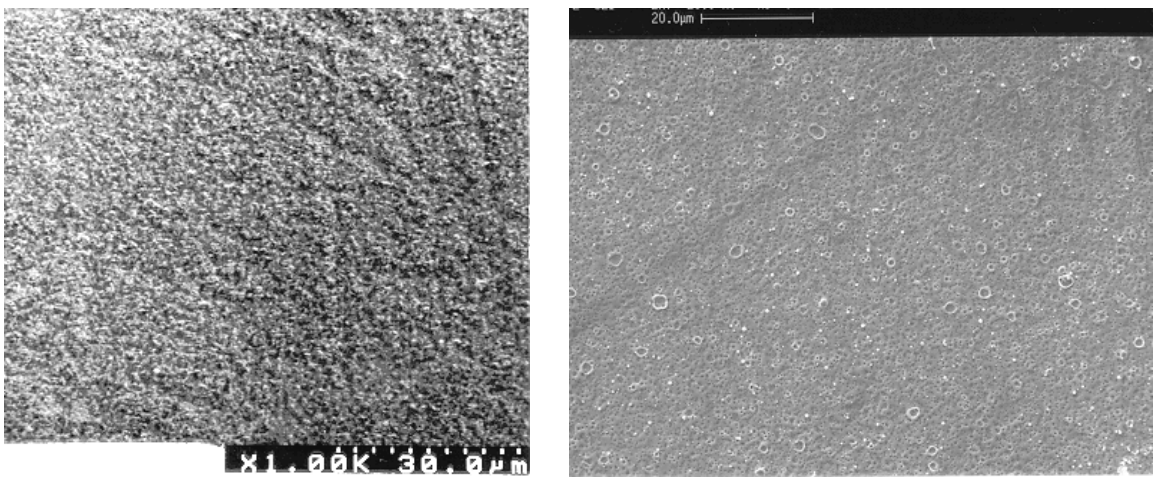

Fig. 4: SEM micrographs of Er_2O_3 deposited onto stainless steel and H-13 steel.

SUMMARY AND CONCLUSIONS

We have deposited and studied several materials as liquid-metal corrosion and erosion barriers. Our initial studies indicate that the concept has merit. For one of our material systems, boron carbide, we will have to significantly reduce the hydrogen content. We will adopt the same strategy we used with AlN to reduce the hydrogen content. Much to our surprise, $Cr_{0.44}C_{0.40}O_{0.20}$ showed early promising results. This was not one of our original candidate materials. In addition to reducing hydrogen content, we will include coupling of the two processes.

Development of Improved Refractories

A. A. Wereszczak, K. C. Liu, and B. A. Pint
Metals and Ceramics Division
Oak Ridge National Laboratory
P.O. Box 2008, Oak Ridge, Tennessee 37831

M. Karakus and R. E. Moore
University of Missouri at Rolla
1870 Miner Circle, 222 McNutt Hall
Rolla, Missouri 65409-0330

INTRODUCTION

The goal of the project is to provide expertise and facilities for the high-temperature mechanical properties characterization of refractory materials that are of interest to the U.S. Department of Energy's Office of Industrial Technologies Advanced Industrial Materials Project. The project dedicates refractory-testing facilities capable of generating representative engineering creep data at temperatures up to 3200°F (1750°C) in ambient air. The generated data serve R&D requirements of refractories manufacturers and the glass-manufacturer end users and designers. The relevance of this effort to the refractory and glass-making industries is ensured by (1) coordinating our research activities with the Glass Industry Advisory Committee (GIAC), which comprises recognized technical representatives from refractory vendor and glass-manufacturing companies; (2) receiving input from key representatives and furnace refractory specialists from the glass-manufacturing community; and (3) subcontracting with the University of Missouri-Rolla (UMR), whose reputation in refractory research is internationally recognized.

Valid engineering creep data do not exist currently for almost all commercial refractories. Refractory end users such as glass-manufacturers require such data for (1) comparing competing brands in their choice of refractories for glass-furnace construction and (2) efficiently and economically designing their various glass-melting furnace superstructures. Refractories in glass-production furnaces may be subjected to extreme temperatures as high as 1750°C. With the simultaneous imposition of mechanical and thermal stresses, creep deformation of the refractory material occurs as a consequence. Designers must ensure that the structural integrity is maintained for optimal service, so these high-temperature deformations must be considered for successful glass-furnace superstructure design. These criteria can be satisfied only with the utilization of representative engineering creep data for the refractory materials that are chosen for the design of the refractory superstructures.

The high-temperature refractory testing facilities are equipped with instrumentation to accurately control and monitor refractory creep tests. Two test frames are being used for the project. Each testing station consists of a testing frame, a computer and appropriate software for test control and data acquisition, a furnace and load train capable of achieving and maintaining loads and temperatures to 3200°F, and a high-temperature

extensometer to monitor strain as a function of time or stress. High-temperature test conditions will be selected that mimic those of refractory service (determined through consultation with the GIAC). Success of this subtask will be demonstrated when representative engineering creep data become available to those scientists, engineers, technicians, and academicians requiring the information for use in refractory materials development and furnace superstructural design.

TECHNICAL PROGRESS: FY 1998

The compression creep and corrosion-resistance performance of the conventional silica refractory category was completed. This work comprised almost all the efforts in FY 1998. The results and conclusions are described below.

Six silica brands were analyzed. The amount of compressive creep of Gen-Sil, Stella GGS, Vega, Vega H, and Harbison-Walker's new developmental brand of conventional silica was negligible at temperatures of 1550 to 1650°C (2820 to 3000°F) and at compressive stresses of 0.2 to 0.6 MPa (29 to 57 psi). The compressive creep of SI96AU conventional silica was negligible at 1550°C. However, SI96AU deformed (contracted) by more than 20% at 1600°C at stresses of 0.2 to 0.6 MPa, a property that was inferior to that of the other five brands tested. SI96AU was not creep tested at 1650°C; however, its creep deformation still was expected to be inferior to the other five silica brands.

The compressive creep rates of all six brands could not be represented as a function of temperature and compressive stress using the conventional Arrhenius Norton-Bailey creep equation (i.e., the Arrhenius power-law creep model). Concurrently active mechanism(s), other than creep, resulted in larger dimensional changes than those produced by creep; this effect limited the ability to identify or interpret the lesser-active creep mechanism in these silica refractories.

Unexpectedly, the change in dimensions of the compressively crept specimens indicated that their size (both diameter and length) had actually *increased* as a consequence of the employed creep-test conditions. All six brands showed this expansion effect. The increases in diameter and length of the creep specimens were between 0.35 to 1.0%. Only a fraction of this expansion was detected during the compressive creep testing. This indicates that most of the permanent expansion exhibited by these silica refractory creep specimens occurred during their heating from ambient to the creep-testing temperature or during the cooling from it to ambient.

The secondary phase constituents remained in all brands when they were tested at 1550°C (cumulative time at temperature approximately 250 h). A fraction of these phases visibly evolved from the specimens at 1600°C (slight glass bubbling on the specimen and fixturing). This phenomenon was quite severe at 1650°C. The density changes in the crept specimens (a net effect of the volume expansion and loss in secondary phase mass) ranged from a decrease of 1.6 to 3.9% with a subtle trend of greater density decreases at higher test temperatures. The density decreases among the six brands were statistically equivalent within the data scatter.

Unstressed or "aging" silica refractory specimens from all six materials also exhibited loss of mass, dimensional increases, and density decreases at 1550 to 1650°C.

- The mass losses of the six brands at 1550 and 1600°C were equivalent; however, some silica brands lost more mass than others at 1650°C: Harbison-Walker's developmental brand lost approximately 0.1% of its mass; SI96AU lost ≈0.2%; Vega H lost ≈0.3%; Gen-Sil lost ≈0.5%; Vega lost ≈1.0%; and Stella GGS lost ≈1.5%. The majority of the mass loss for all six brands occurred in less than 25 h.
- The dimensional increases of the silica specimens were a function of temperature. Additionally, some brands expanded more than others. The ranges of expansion were ≈1 to 2.5% at 1550°C, ≈2.25 to 3.75% at 1600°C, and ≈3.5 to 6% at 1650°C. Harbison-Walker's developmental brand expanded the least amount at all three temperatures, followed by Gen-Sil. The ascending order of expansion for the other four brands varied with temperature. Stella GGS expanded the most at 1550°C (≈2.5%), SI96AU expanded the most at 1600°C (≈3.75%), and Vega expanded the most at 1650°C (≈6%). Dimensional increases in these aging specimens were greater than axial expansion of the crept silica specimens at the same temperatures, indicating that the axially applied compressive load during creep testing resulted in *some* specimen contraction.
- The density decreases of the silica specimens were a function of temperature. Additionally, some brands became less dense than others. The changes in density were a consequence of the above described changes in mass and volume. The ranges of density decreases were ≈1 to 2.75% at 1550°C, ≈2.25 to 4.0% at 1600°C, and ≈3.5 to 7.0% at 1650°C. The density of Harbison-Walker's developmental brand changed the least of the six brands at all three temperatures. The ascending order of density for the other five brands varied with temperature. The density of Stella GGS decreased the most at 1550°C (≈2.75%), that for SI96AU decreased the most at 1600°C (≈4%), and that for Vega decreased the most at 1650°C (≈7%).

The corrosion-resistance data of the six brands were equivalent (i.e., exhibited equivalent amounts of recession using ASTM C987 lid test) when they were subjected to sodium carbonate vapors at 1400°C (2550°F).

MILESTONES

Completed compressive creep testing of conventional silica refractories (9/98).

PUBLICATIONS

A. Wereszczak, "Which Superstructure Refractories Do Glassmakers Desire Creep Data For?" *Glass Industry*, pp. 17–18 and 24, (November 1998). Note that this was submitted for publication in FY 1998, but it was published in early FY 1999.

Journals

None.

Other Publications

None.

PRESENTATIONS

Oral Presentations

"Characterization of Refractories for the Glass Manufacturing Industry," *1998 Glass Industry Project Review*, Argonne, Illinois, August 12, 1998.

"Development of Improved Refractories," *3rd Annual OIT/AIM Program Review*, Jackson Hole, Wyoming, June 24, 1998.

HONORS AND AWARDS

None.

PATENTS/DISCLOSURES

None.

LICENSES

None.

INDUSTRIAL INPUT AND TECHNOLOGY TRANSFER

Two GIAC meetings were held in FY 1998 (13Oct97 and 23Mar98). The committee critiqued the project's efforts and provided guidance and suggestions for ongoing and anticipated future refractories research.

ESTIMATED ENERGY SAVINGS

Based on the *1998 DOE/OIT GPRA Report*, approximately $202M in energy savings per year in 2005 and a $445M per year savings by 2020 are anticipated with the conversion of air/fuel- to oxy-fuel–fired glass-manufacturing furnaces. These are quoted results from the consideration that 61% and 100% furnace conversions will occur by the years 2005 and 2020, respectively. Glass manufacturers and their furnace designers will use the results from this project to accelerate this conversion process to achieve these energy realizations.

Materials R&D—Student Internships

R. B. Thompson, I. E. Anderson, and T. E. Bloomer
Ames Laboratory
Iowa State University, Ames Iowa 50011

INTRODUCTION

This program's objective is to conduct programmatic research for the Advanced Industrial Materials Program while training minority students at the same time. Well-known demographics indicate that minorities will constitute an increasing fraction of our future work force. Consequently, efforts have been initiated to increase the fraction of minorities and women who choose and successfully follow technical career paths. Included are a wide-ranging set of programs, beginning with preschool education, progressing through efforts to retain students in technical paths in grades K–12 and undergraduate education, and ending with encouraging graduate education. The Materials R&D—Student Internships is a unique approach in the latter category. Here, we have focused on a particular area of applied materials research in the AIM Program. Our goal, then, is to educate minority graduate students in the context of this program. The Ames Laboratory was selected as a site for this pilot project because it is a DOE national laboratory located on the campus of a major research university and includes programs that have a strong technological flavor in their research interest. Many of the Ames Laboratory staff hold shared faculty appointments.

More specifically, the pattern through which a student will pass involves a sequence of steps progressing through recruitment, project selection, research, mentoring, and graduation. Recruiting is being accomplished by national advertising of the AICD Materials Technology Fellowships for Minorities. We feel that it would be desirable to offer at least one such fellowship each year to maintain continued visibility on minority campuses and to establish effective working relationships with appropriate personnel. Other factors that we believe to be essential for the success of the project include offering each student a variety of project opportunities—active choice in project selection will greatly increase the student's motivation and likelihood of success—and continued mentoring throughout the program. The projects offered to the students are consistent with the guidelines of the AIM program.

TECHNICAL PROGRESS: FY 1998

During FY 1998, our third student, Ms. Tamara E. Bloomer, began studies toward her Master's Degree in Materials Science. Her work concerns the microstructural and mechanical properties of SnAgCu+Co, a new lead-free solder. Technical progress on her project is summarized below.

For electrical circuitry in the harsh environments of cars and airplanes, mechanical durability and elevated temperature performance of solder joints are of paramount importance to prevent electronic system failure. These characteristics are promoted by proper design of the solder alloy to promote microstructural strength and stability in the

solder joint. It has been shown that formation of intermetallics at the solder/substrate (typically Cu) interface improves the wetting characteristics of most Sn-based solders. Promoting wetting is especially important in the development of Pb-free replacements for Sn-Pb eutectic solder, which is noted for excellent wetting. A few years ago, a Sn-4.7Ag-1.7Cu (wt %) ternary eutectic solder alloy was demonstrated to have very good wetting cabilities, relative to the other Pb-free solder candidates. However, some concern was reported about the microstructural integrity of the interface between the intermetallics and the solder matrix resulting from the weakness of the faceted intermetallic interface during tensile testing of this alloy. Although shear stress, and not tensile stress, is probably a more common cause of mechanical failure in solder joints, the faceted intermetallic interface appears to be an important microstructural weakness to mitigate in Sn-Ag-Cu solders, as well as in other Sn-base solders. This investigation was begun to modify the faceting tendency of the intermetallic interface phase by transition metal additions (primarily Co, Ni, and Fe) to Sn-Ag-Cu eutectic and near-eutectic solder alloys.

Preliminary solder-wire tensile testing suggested that small amounts (<0.5 wt %) of Co or Ni improved the strength of the Sn-Ag-Cu eutectic and near-eutectic solder. The current study established that additions of Co, Ni, and Fe enhanced the retention of strength in Sn-Ag-Cu solder alloys that were subject to extended high-temperature annealing (170ºC, 14 h). Microstructural analysis revealed an increased refinement of the as-solidified solder microstructures of the Ni- and Co-modified alloys and retention of this reduced microstructural scale after annealing, consistent with the strength results. Initial observations of model solder-joint microstructures indicated that the Co addition had the most profound effect on supressing intermetallic faceting in both of the as-solidified samples, even after extended high-temperature annealing, see Fig. 1. Subsequent solder-joint samples have been prepared for shear-strength evaluation by a newly developed asymmetric four-point bend (AFPB) test. A limited set of Co- and Ni-modified Sn-Ag-Cu solder alloys will be compared with a representative collection of competing solder alloys (e.g., Sn-Ag, Sn-Cu, and Sn-Pb eutectics) in this and other mechanical-property evaluations. Initial AFPB tests using a Sn-Ag eutectic solder alloy as a reference have established that a solder joint gap of 0.076 mm should be used for preparation of all of these butt-joint samples. A full set of AFPB specimens will be prepared in the next reporting period and used for evaluation of ambient and elevated temperature shear strength. To examine the fatigue performance over a useful temperature range, thermal-mechanical fatigue tests will be performed over a range of –55 to 150°C with the same set of alloys.

MILESTONES

Microstructural analysis of a new lead-free solder family will be conducted to explore the effects of alloying elements on microstructural stability of the solder and solder-joint samples at temperatures above 150°C (September 1999 completion).

Solder-wire tensile strength of the new solder alloys will be studied (July 1999 completion).

Asymmetric four-point bend testing of butt-joint samples will be studied to obtain shear strength measurements of the solder joint samples (July 1999 completion).

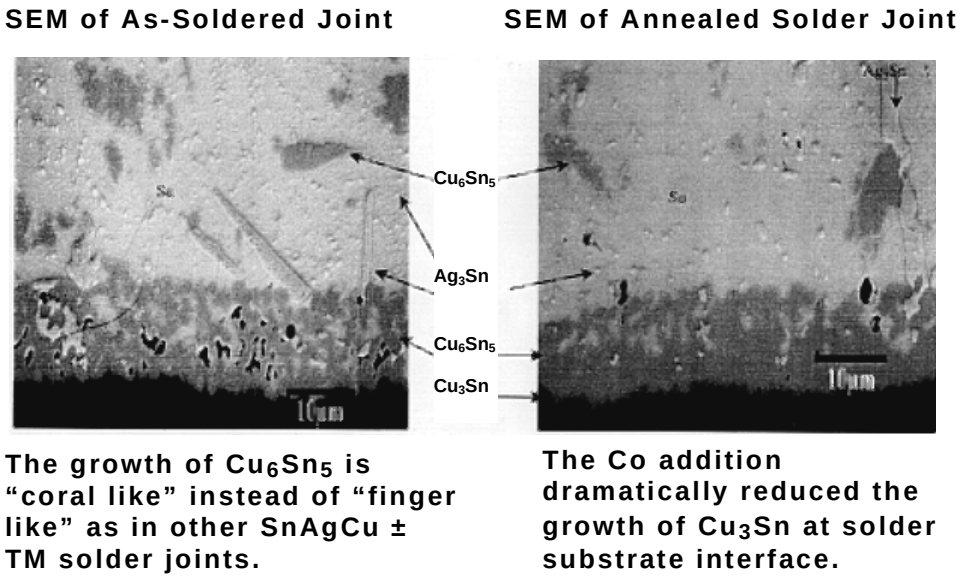

Fig. 1. Model solder-joint microstructures show effect of Co addition on supressing intermetallic faceting on both samples.

We will subject thermal-mechanical fatigue specimens to temperature cycles and periodically analyze their microstructures to determine failure onset and microstructural mechanisms (December 1999 completion).

PUBLICATIONS

E. Anderson, O. Unal, T. E. Bloomer, and J. C. Foley, "Effects of Transition Metal Alloying on Microstructural Stability and Mechanical Properties of Tin-Silver-Copper Solder Alloys," in *Proceedings of The Third Pacific Rim International Conference on Advanced Materials and Processing (PRICM 3)*, 2, The Mineral, Metals & Materials Society, 1998, p. 189.

PRESENTATIONS

I. E. Anderson, O. Unal, T. E. Bloomer and **J. C. Foley**, "Effects of Transition Metal Alloying on Microstructural Stability and Mechanical Properties of Tin-Silver-Copper Solder Alloys," The Third Pacific Rim International Conference on Advanced Materials and Processing (PRICM 3).

Student Oral Presentations

Microstructural Evolution of Lead Free Solders During Annealing, **T. E. Bloomer**, I. E. Anderson, J. C. Foley, R. Terpstra, and E. Eckhart, Advanced Materials Conference, Jackson Hole, Wyoming, June 22, 1998.

HONORS AND AWARDS

None.

PATENTS/DISCLOSURES

None.

LICENSES

None.

INDUSTRIAL INPUT AND TECHNOLOGY TRANSFER

Multicore Solders, Hector Steen
Johnson Manufacturing, Al Gickler
Nihon Superior, Tetsuro Nishimura

ESTIMATED ENERGY SAVINGS

None.

Metals Processing Laboratory User (MPLUS) Facility

Gail Mackiewicz-Ludtka and H. W. Hayden
Oak Ridge National Laboratory
P.O. Box 2008, Oak Ridge, Tennessee 37831

INTRODUCTION

The Metals Processing Laboratory User (MPLUS) Facility, officially designated as a DOE User Facility in February 1996, continues to be a success after more than 2 years. Its primary purpose is to assist researchers in key U.S. industries, universities, and federal laboratories in improving energy efficiency and enhancing U.S. competitiveness in the world market. The MPLUS Facility provides users the unique opportunity to address technology-related issues to solve metals-processing problems from a fully integrated approach. DOE facilitates the process and catalyzes industrial interactions that enable technical synergy and financial leveraging to take place between the industrial sector, which is identifying and prioritizing its technological needs, and MPLUS, which provides access to the technical expertise and specialized facilities to address these needs.

MPLUS was designed to provide U.S. industries with access to the specialized technical expertise and equipment needed to solve metals-processing issues that limit the development and implementation of emerging metals-processing technologies. As originated, MPLUS includes the following four primary user centers: Metals Processing, Metals Joining, Metals Characterization, and Metals Process Modeling. These centers are devoted to assisting U.S. industries in adjusting to rapid changes in the marketplace and in improving products and processes. This approach optimizes the complementary strengths of industry and government. Tremendous industrial response has resulted in MPLUS expanding to meet the ever-growing technical needs and requests initiated by U.S. industry.

TECHNICAL PROGRESS: FY 1998

Summary

1. From the official designation of MPLUS as a DOE User Facility on February 9, 1996, MPLUS has grown continuously, primarily responding to industrial needs and requests. MPLUS has grown from representing initially only the Engineering and Materials Section within Oak Ridge National Laboratory's (ORNL) Metals and Ceramics Division (M&C), to include other ORNL User Facilities now as well. MPLUS expanded first to include other User Facilities within M&C [e.g., the High Temperature Materials Laboratory (HTML)] and then to include additional User Facilities within other ORNL divisions [e.g., the Computational Center for Industrial Innovativeness (CCII)], and facilities beyond ORNL. Based upon the needs and requests from industry, MPLUS has provided industries and academia with access to unique capabilities and technologies beyond those originally designated within ORNL as DOE User Facilities (e.g., the Microwave Facilities within the ORNL

Fusion Energy Division). In fact, with the growing response and needs being identified, MPLUS has become a viable vehicle/mechanism to unite other national laboratory User Facilities to provide industry with a mechanism to access these national resources as a *Distributed Laboratory*.

2. As of September 30, 1998, a total of 107 MPLUS proposals were received from 60 different companies and universities representing states across the United States (Fig. 1). Many additional companies representing several other states also have expressed interest in MPLUS and have submitted proposals. However, in several cases (four in FY 1998 alone), upon further discussions with some companies, agreements other than User Agreements are found to be more suitable to their needs, and these companies then pursue other types of agreements. The demand for and success of the MPLUS User Facilities continues. The demand for and success of MPLUS are evidenced by (a) the sheer number of users (61 companies); (b) the significant numbers of organizations (19) who requested repeated assistance and submitted multiple (2 to 5) proposals for different MPLUS projects; (c) the four companies who chose to do proprietary MPLUS projects, with 2 of these 4 users pursuing multiple proprietary MPLUS projects.

3. Of the 107 proposals received, 78 have been reviewed, and **59** *of these 78* ***MPLUS User projects have been initiated.***

4. As of September 30, 1998, ***21*** MPLUS projects were ***completed.***

Industry and academia had demonstrated such a positive response to the MPLUS Program and Facilities that the demand actually exceeded the supply of resources by May 1998. Consequently, as of May 1998, no new MPLUS projects could be accepted for FY 1998 funding.

MILESTONES

FY 1998

Leveraged funding and capabilities with other DOE/OIT/AIM programs	FY 1998
Developed an ORNL report (ORNL/M-6385) detailing as well as summarizing MPLUS capabilities	February 1998
Developed drafts of MPLUS Project Summary Books for each individual Vision Industry (VI)	March 1998
Developed and implemented PC & Mac availability of MPLUS proposals on the Internet	April 1998
Developed and updated a draft version of the MPLUS VI Summary Notebook	June 1998

FY 1997

Developed a 1-Page MPLUS Summary Sheet	May 1997

Developed an MPLUS Vision Industry Summary Notebook	June 1997
Investigated partnering with non-ORNL facilities *(Adv. Steel Processing Center)*	June 1997
Developed Internet-downloadable version of Proposal form (*http://www.ms.ornl.gov/emfacility/mplus/forms.htm)*	September 1997
Initiated 53 MPLUS proposals (48 nonproprietary and 5 proprietary)	September 1997
Completed 10 MPLUS projects (1 proprietary)	September 1997

FY 1996

Designated as a DOE User Facility	February 1996
Developed Program methodology and database	March 1996
Developed User Brochure	April 1996
Put user information on Internet and initiated 15 vision industry proposals	June 1996
Drafted first Business Management Plan	July 1996

PUBLICATIONS

"DOE User Facilities and Capabilities," submitted to be published in the ASM proceedings from their Annual Review Meeting as part of the ASM–Heat Treat Symposium, October 1998.

Summary Binder of MPLUS User Projects according to Vision Industry, June 1998.

Metals Processing Laboratory Users Facility Report, ORNL/M-6385, February 1998.

Metals Processing Laboratory Users Facility Report, ORNL/M-4466, 1997.

Summary Binder of MPLUS User Projects according to Vision Industry, June 1997.

"MPL U.S. DOE User Facilities Summary Sheet," May 1997.

Internet Information/Web Pages, updated May 1997 (URL: http://www.ms.ornl.gov/emfacility/mplus/mplus.htm).

MPLUS User Program brochure, updated April 1997.

Metals Processing Laboratory User Facility-Facilities Capabilities, Interactive Programs, and Recent Experience, ORNL Internal Report, March 1997.

Oak Ridge User Facilities pamphlet, Summer 1996, pp. 16–17.

Internet Information/Web Pages, updated May 1996 (URL: http://www.ms.ornl.gov/emfacility/mplus/mplus.htm).

MPLUS User Program, brochure, developed April 1996.

"MPLUS Center Welcomes First Industrial User," *The M&C Pipeline*, published by the Metals and Ceramics Division, **5**(2), 10 (March/April 1996).

PRESENTATIONS

Numerous posters and presentations were given informally at various on-site (ORNL) and off-site meetings. These included posters and presentations to various DOE officials and groups, the ASERTTI Group representing States, the Metal Casting Showcase and Exhibition, international groups (e.g., Norway visitors), and various technical association groups (e.g., The Aluminum Association). The more formally organized presentation and poster sessions are detailed below:

Poster Sessions

"Metals Processing Laboratory User Facility," Oak Ridge National Laboratory User Facility, for Poster Session at 1998 ASM Annual Meeting/ASM-Heat Treat Symposium and Exposition, Illinois, October 1998.

"Metals Processing Laboratory User Facility," Oak Ridge National Laboratory User Facility, for Poster Session at 1998 Advanced Industrial Materials (AIM) Program Annual Meeting in Jackson Hole,Wyoming, June 24–26, 1998.

"Metals Processing Laboratory User Facility," Oak Ridge National Laboratory User Facility, for Poster Session at 1997 Advanced Industrial Materials (AIM) Program Annual Meeting in Albuquerque, New Mexico, June 16–18, 1997.

"Metals Processing Laboratory User Facility," Oak Ridge National Laboratory User Facility, for Poster Session AIM booth at the OIT Exposition, October 1998.

"Metals Processing Laboratory User Facility," Oak Ridge National Laboratory User Facility, for Poster Session for the ASM Materials Exposition at the 1997 ASM/AIME Annual Technical Meeting, October 1997.

"Metals Processing Laboratory User Facility," Oak Ridge National Laboratory User Facility, for Poster Session at Advanced Industrial Materials (AIM) Program Annual Meeting in Pollard Auditorium, Oak Ridge, Tennessee, June 24–26, 1996.

Informal oral presentations and tours

"Metals Processing Laboratory Users Facility (MPLUS)," for visit by VI Staff visitors, Spring, 1998.

"Metals Processing Laboratory Users Facility (MPLUS)," for visit by Ford Motor Co. Rough Part Forming Forum, emphasis on Metal Casting & Forging, October 8, 1997.

Metals Processing Laboratory Users Facility (MPLUS)," for visit by Sara Dillich Program Manager of the Aluminum Vision Industry Team for DOE/OIT, emphasis on Aluminum & Metal Casting, October 2, 1997.

"Metals Processing Laboratory Users Facility (MPLUS) Update," for Program Managers (Tony Schaffhauser and Mike Karnitz) Meeting, July 25, 1996.

"Overview of the Metals Processing Laboratory Users Facility (MPLUS)," for the directors and staff members of ten State Energy Offices, as well as representatives from the Southern States Energy Board, the Harmony Project from Charleston, South Carolina, and the DOE Atlanta Regional Support Office, November 20, 1996.

"Metals Processing Laboratory Users Facility (MPLUS)," for DOE/OIT, Bill Parks and Charles Sorrell, December 5, 1996.

Honors And Awards

November, 1996: The President's Award for Continuous Improvement for the MPLUS Users Facility—Metals Processing Users Project

LICENSES

None.

INDUSTRIAL INPUT AND TECHNOLOGY TRANSFER

As of September 30, 1998, a total of 107 MPLUS Proposals were received from 60 different companies and universities representing states across the United States (Fig. 1). Many additional companies, representing several other states, also have expressed interest in MPLUS. The demand and success of MPLUS are evidenced by (a) the sheer number of users (60 companies); (b) the significant numbers of organizations (19 different ones) who have requested repeated assistance and submitted multiple (2 to 5) proposals for different MPLUS projects; (c) the 4 companies who chose to do Proprietary MPLUS projects, with 2 of these 4 users pursuing multiple proprietary MPLUS projects.

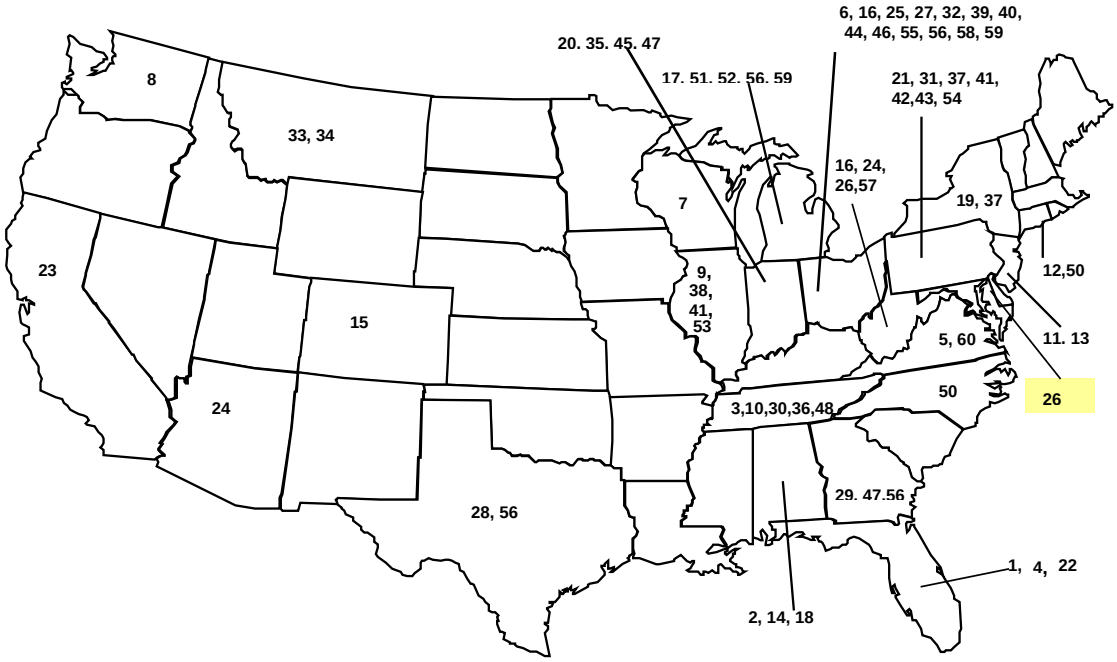

1. Westinghouse (2)
2. Reynolds (3)
3. ForMat Industries
4. U.S. Filter
5. E.R. Johnson
6. Sandusky Int'l
7. Waukesha Electric
8. Weyerhauser (2)
9. A. Finkl (3)
10. Jeffrey Chain Corp
11. Materials Tech.
12. ABB C-E Serv. (3)
13. Union Camp Corp
14. United Defense (2)
15. CO School of Mines
16. Weirton Steel
17. General Motors (2)
18. Univ. of AL (2)
19. Cornell Univ.
20. Cummins Engine (3)
21. Bethlehem Steel (2)
22 Anchor Glass
23. FMC Corp.
24. WV Univ. (2)
25. Dana Corp.
26. Westvaco
27. Lincoln Electric
28. CarboMedics
29. IPST
30. Univ. of Tenn.
31. PPG industries (4)
32. Owens Corning (2)
33. Columbia Falls AL
34. AFFCO
35. Allison Engine
36. TTE
37. Alcoa Al
38. Wagner Castings
39. Rhenium Alloys
40. Uniform Metal Tech
41. Univ. of Pittsburgh
42. J&L Specialty Steel
43. Penn State Univ.
44. Finite Solutions
45. Caterpillar
46. General Electric
47. Southwire Co.
48. Smelter Services
49. Stoody
50. Torrington (2)
51. Ford Motor Co. (3)
52. Eaton(2)
53. Hoskins Mfg. (2)
54. AHT Inc.
55. DCT, Inc.
56. Amercord
57. INCO Alloys Int'l (5)
58. LTV Steel
59. Amer. Axle
60. Vir. Poly.& St. U.

Fig. 1. As of September 30, 1998, a total of 107 MPLUS proposals were received from 60 different companies and universities representing many states across the United States.

Microwave Joining of SiC

R. Silberglitt and G. A. Danko
FM Technologies, Inc.
10529-B Braddock Road
Fairfax, Virginia 22032

P. Colombo*
University of Padua
via Marzolo 9
35131 Padua, Italy

INTRODUCTION

The purpose of this work is to optimize the properties of SiC-SiC joints made using microwave energy. The current focus is on identification of the most effective joining methods for scaleup to large tube assemblies, including joining using SiC produced in situ from chemical precursors.

During FY 1998, a detailed investigation was performed of the SiC product produced from several different commercially available polymer precursors, in order to assess their relative usefulness as filler materials for microwave joining. In addition, by comparing these results with those of parallel experiments that were performed at the University of Padua using conventional heating, direct comparisons were obtained of the SiC product formed from each precursor processed via the two different heating methods.

A determination also was made of the shrinkage during pyrolysis and annealing of neat and SiC particulate–loaded allylhydridopolycarbosilane (AHPCS) polymer. This polymer was used to join sintered SiC tubes, which were 8 in. long, with 1-in. outer diameter and 1-in. inner diameter collars, that were tested to failure at the ORNL High Temperature Materials Laboratory (HTML) at ambient temperature and 1050°C, with all failures in the tubes and collars and no failures in the joint. These data are necessary input to a stress analysis of the three-dimensional (butt-plus-lap) joints.

TECHNICAL PROGRESS: FY 1998

Summary

Comparison of microwave and conventional processing of polymer precursors

A detailed investigation was performed of the SiC product produced from several different commercially available polymer precursors, in order to assess their relative usefulness as filler materials for microwave joining. In addition, by comparing these results with those of parallel experiments that were performed at the University of Padua using conventional heating, direct comparisons were obtained of the SiC product formed

*Present Address: University of Bologna, viale Risorgimento 2, 40136 Bologna, Italy.

from each precursor processed via the two different heating methods. The materials used in this investigation were as follows:

- SR-350, silicone resin available from GE;
- SR-355, silicone resin with excess C available from GE;
- PCS, polycarbosilane available from Nippon Chemicals;
- D-PPC, polycarbosilane with excess C available from Solvay;
- AHPCS, allylhydridopolycarbosilane available from Starfire Systems;
- AHPCS, with addition in the laboratory of 1 wt % nanosize (<20 nm) SiC powder; and
- Ceraset SN™, available from Allied Signal Composites.

Identical quantities of each of these materials from the same lot were cross-linked using a 0- to 6-kW 2.45-GHz microwave source, together with a 40.6-cm (16-in.) by 40.6-cm (16-in.) multimode applicator and an insulated enclosure lined on the inside with a thin layer of SiC to provide hybrid (microwave plus radiant) heating. Five-gm quantities of the SR-350, SR-355, PCS, DPPC, and AHPCS were placed into Pyrex (borosilicate) test tubes. In addition, 5 gm of AHPCS was mixed with 0.05 gm of nanosize SiC powder, and 5 gm of Ceraset SN was mixed with 0.05 gm of dicumyl peroxide (a recommended cross-linking agent). These mixtures also were each placed into Pyrex test tubes. The test tubes were placed inside the hybrid heating enclosure, the applicator was slowly pumped to 2×10^{-2} torr, then backfilled with argon to –482 mm (19 in.) Hg. The applicator was pumped again to 2×10^{-2} torr, and the microwave power was turned on. The specimens were heated to a temperature of 400°C at a rate of 1 to 2°C per min, and then from 400 to 600°C at a rate of approximately 5°C per min. The applicator was back-filled with argon after the specimens had reached a temperature of 450°C. The applicator was allowed to cool and the specimens, which were now cross-linked, were removed.

The cross-linked specimens of each material were separated into five groups, each of which was pyrolyzed and annealed to a different temperature: 1100°C, 1200°C, 1300°C, 1400°C, and 1500°C. For these pyrolysis and annealing steps, the specimens were contained in quartz cuvettes, which were placed inside the hybrid heating enclosure inside the multimode applicator. The applicator was pumped to a pressure of 10^{-2} torr before processing. Heating was under vacuum at 2°C per min up to 600°C, and under argon overpressure at 10°C per min to annealing temperature. The specimens were held at the annealing temperature for 30 min. Temperature was monitored using a two-color optical pyrometer, as well as a type-K thermocouple, which was inserted into the center of the hybrid heating enclosure. The specimens were weighed both before and after processing to allow determination of percentage weight loss. After processing, the specimens were sent to the University of Padua.

At the University of Padua, identical specimens of all of the polymers were processed using conventional heating. The specimens were inserted in alumina boats and heated at

10°C per min in an alumina tube furnace under flowing argon. The samples were isothermally held for 30 min at temperatures ranging from 1000 to 1500°C. The specimens were weighed both before and after processing to allow determination of percentage weight loss.

The crystallinity of the materials was detected by X-ray diffraction (XRD) at the University of Padua using a Philips PW1820 diffractometer (CuKα radiation, 40 kV, 40 mA). The average crystallite sizes were calculated using the Scherrer equation; for the microstructural characterization, an improved profile-fitting method using a pseudo-Voigt representation for the line profiles was used. The same amount of material was investigated for each specimen (about 500 mg), and a comparative semi-quantitative evaluation of the amount of SiC phase formed was performed by measuring the area under the main peak located at ~35.6° 2θ (<111>, β-SiC, JCPDS card #29-1129). Analysis of these data revealed that β-SiC was the only crystalline phase formed, and that both the amount of crystalline material and the crystallite size increased with annealing. The average crystallite sizes for the polysiloxanes and Ceraset SN are shown in Fig. 1, and those for the polycarbosilanes are shown in Fig. 2.

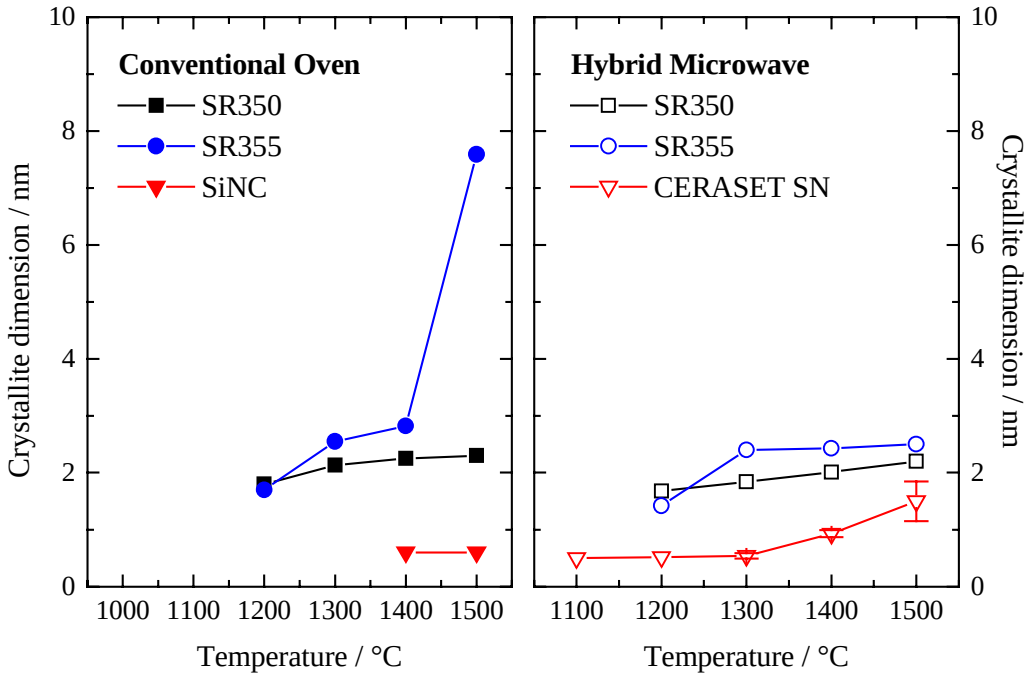

Fig. 1. Crystallite dimensions of SiC produced from polysiloxanes and Ceraset SN, as determined by X-ray diffraction.

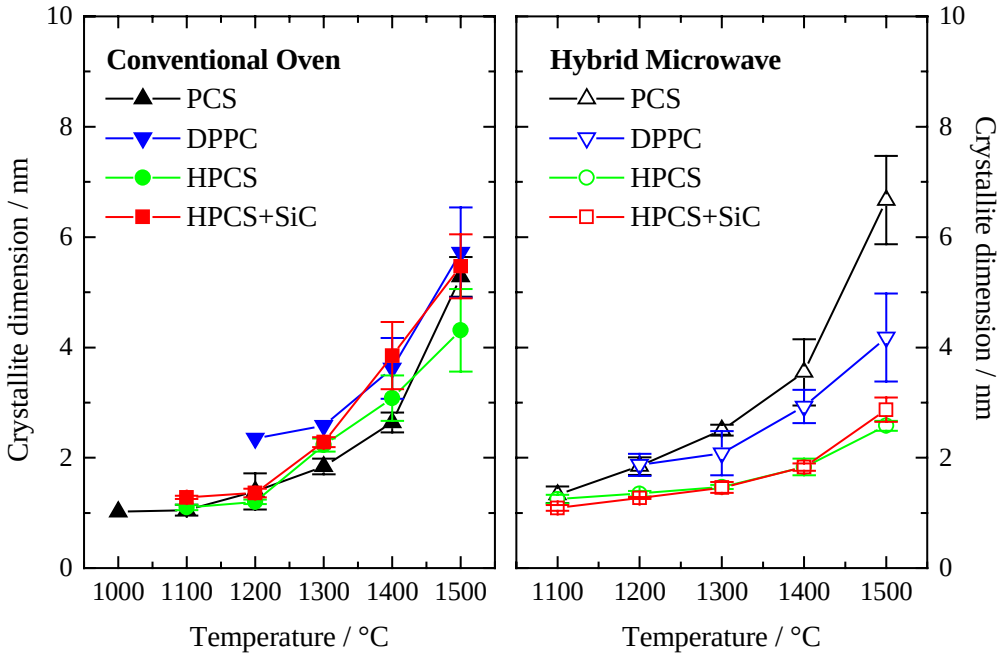

Fig. 2. Crystallite dimensions of SiC produced from polycarbosilanes, as determined by X-ray diffraction.

The β-SiC crystallite size for all materials ranged from 2 to 8 nm, with small differences between the heating methods, except for SR-355 at 1500°C and Ceraset SN. Pyrolysis of SR-350 and SR-355 produces SiOC, which then converts to β-SiC. At low temperatures, the formation of SiC within the amorphous matrix is mainly a result of Si-O and Si-C bond redistribution to form SiC and SiO_2. For pyrolysis temperatures higher than about 1400°C, carbothermal reduction starts to play an important role, leading to the formation of more SiC phase. It is believed that the flowing argon atmosphere in the conventional oven promoted carbothermal reduction, leading to higher levels of β-SiC from SR-355 at 1500°C. For the Ceraset SN, microwave heating appears to produce crystalline material above about 1300°C, whereas the conventional heating did not. For the polycarbosilanes, there was a larger difference in crystallite sizes produced from the different polymers by microwave heating than conventional heating, and the largest crystals were produced by microwave heating of PCS.

Figures 3 and 4 are plots of the area under the main SiC peak, for the polysiloxanes and Ceraset SN and the polycarbosilanes, respectively. This area provides a qualitative estimate of the amount of crystalline SiC formed. The higher values for SR-355 by conventional heating and Ceraset SN for microwave heating are consistent with the data shown in Fig. 1. For the polycarbosilanes, the differences between the amount of crystalline SiC formed by microwave and conventional heating appear to be dependent upon the amount of carbon in the polymer. For D-PPC (78 wt % C), substantially more SiC was formed via microwave heating. For PCS (37.5 wt % C), only slightly more SiC was formed via microwave heating. For HPCS (28 wt % C), more SiC was formed via conventional heating. Moreover, the addition of SiC powder to the HPCS made no difference for conventional processing but

increased the amount of SiC produced by microwave processing to about the same value as for conventional processing. It appears from these data that the presence of microwave-absorbing material, either in the polymer itself or added as powder, increases the amount of crystalline SiC produced by microwave heating. In fact, in the raw XRD data, the peak from the SiC powder added to the precursor was readily apparent for the conventionally heated material, and appeared to be "washed out" for the microwave-heated material. It is thus hypothesized that in the microwave case, SiC crystals are more effectively nucleated on the powder. Transmission electron microscopy (TEM) measurements are needed to investigate the validity of this hypothesis.

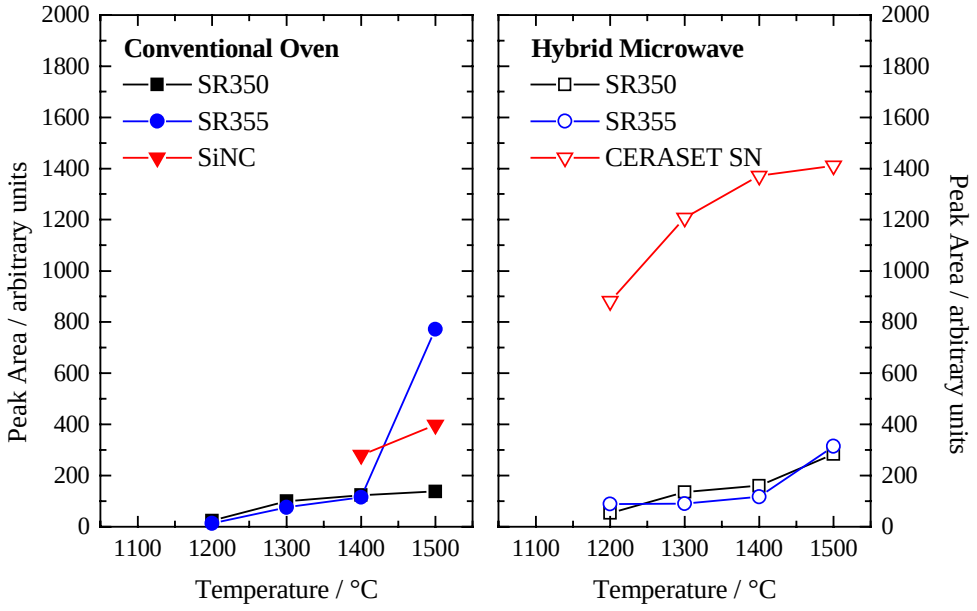

Fig. 3. Peak area of main β-SiC X-ray diffraction peak for polysiloxanes and Ceraset SN.

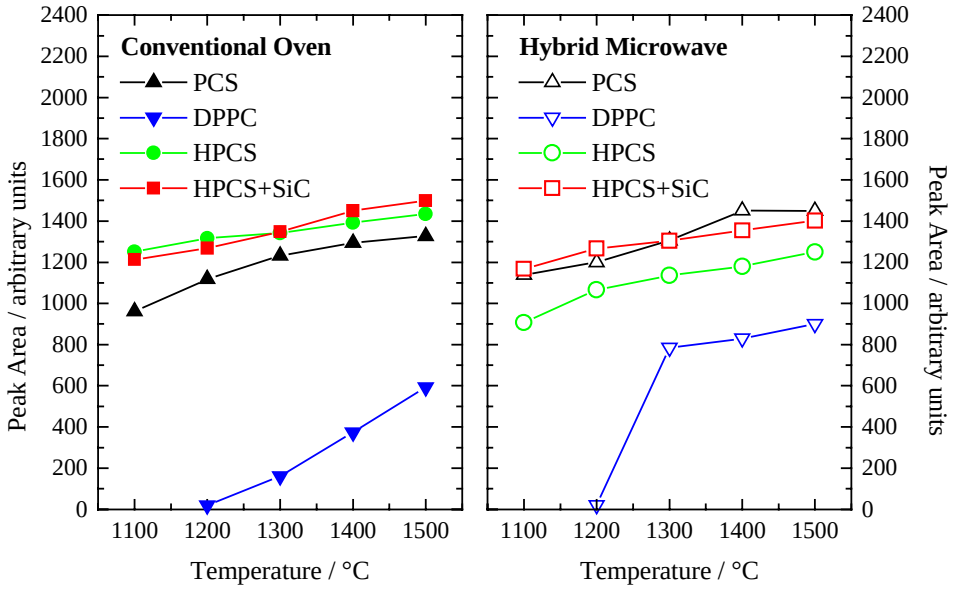

Fig. 4. Peak area of main β-SiC X-ray diffraction peak for polycarbosilanes.

Determination of shrinkage of polymer during pyrolysis and annealing

A known mass and volume of neat AHPCS resin was heated to 600°C using the same microwave hybrid heating technique described above. The sample was allowed to cool and was then removed for weighing. Several large (tens of cubic millimeters) chunks of processed resin were weighed dry, boiled in water, and weighed in a wire basket while immersed. These values were recorded for computation of Archimedes' Density (ρ) using the following relationship:

$$\rho = \text{dry weight} / (\text{dry weight} - \text{wet weight}).$$

From density and total remaining mass, the volume and linear shrinkage were derived.

The specimens were returned to the furnace and heated to 1000°C, after which measurements and calculations were performed as described above. A final anneal at 1380°C was then performed, with measurements and calculations as described above. Volume shrinkage and linear shrinkage for neat AHPCS are presented in Table 1. A shrinkage computation also was performed for SiC powder–loaded slurries according to Rule of Mixtures assumptions. These data are presented in Table 2.

Table 1. Volume and Linear Shrinkage of Neat AHPCS vs Temperature

	600°C	**1000°C**	**1380°C**
Volume Shrinkage	52.9%	67.8%	73.4%
Linear Shrinkage	22.2%	31.5%	35.7%

Table 2: Volume and Linear Shrinkage of SiC-Loaded AHPCS vs Temperature
(Data are normalized to room-temperature starting values, except as indicated.)

	600°C	**1000°C**	**1380°C**
Volume Shrinkage	39.8%	51.0%	55.2%
Linear Shrinkage	15.6%	21.2%	23.5%
Linear Shrinkage relative to 600°C		6.64%	9.39%
Linear Shrinkage relative to 1000°C			2.95%

MILESTONES

Determination of the SiC crystallite size vs processing temperature for polymer precursors with and without SiC particulate loading (June 1998).

1. Comparison of SiC produced via microwave and conventional processing of polymer precursors (June 1998).
2. Determination of the volume and linear shrinkage of neat and SiC-loaded polymer precursor (September 1998).

PUBLICATIONS

"Production of SiC and SiOC From Preceramic Polymers: Comparison of Microwave and Conventional Heating," P. Colombo, G. A. Danko, and R. Silberglitt, *Proceedings of the 9th CIMTEC, World Ceramics Congress & Forum on New Materials*, Florence, Italy, June 14–19, 1998 (in press).

PRESENTATIONS

1. R. Silberglitt and G. Danko, "Recent Results on Microwave Joining of SiC," presented at the BES/CFCC Joining Workshop, CFCC Working Group Meeting, Lake Tahoe, Nevada, October 8, 1997.
2. R. Silberglitt and G. A. Danko, "Joining of Monolithic and CFCC SiC Materials Using Polymer Precursor and Microwave Heating," presented at the 22nd Annual Conference on Composites, Materials and Structures (Restricted Sessions), Cocoa Beach, Florida, January 29, 1998.
3. P. Colombo, G. A. Danko, and R. Silberglitt, "Production of SiC and SiOC from Preceramic Polymers: Comparison of Microwave and Conventional Heating," presented at the 9th CIMTEC, World Ceramics Congress & Forum on New Materials, Florence, Italy, June 19, 1998.
4. R. Silberglitt and G. A. Danko, "Microwave Joining of SiC," poster presented at the Advanced Industrial Materials Annual Review Meeting, Jackson Hole, Wyoming, June 23, 1998.

HONORS AND AWARDS

None.

PATENTS/DISCLOSURES

None.

LICENSES

None.

INDUSTRIAL INPUT AND TECHNOLOGY TRANSFER

An industry-sponsored program is under development with Stone & Webster to join pairs of sintered SiC tube sections to form furnace coils for testing in a prototype high-temperature furnace in an ethylene production plant. Discussions are under way with INEX for application to reaction-bonded SiC radiant burner tube assemblies. Presentations were made at BES/CFCC workshops, and discussions were held with CFCC contractors and program managers.

ESTIMATED ENERGY SAVINGS

Natural gas savings are estimated at $172,892 per year due to 4 to 7% higher efficiency of SiC radiant burner tubes. Use of a SiC tube heat exchanger in externally fired combined-cycle coal power plants is projected to produce a 20% increase in thermal efficiency, together with a 20% reduction in CO_2 emissions and a 90% reduction in SO_x emissions. Energy savings through the reduction of feedstock consumption and decoke fuel and steam requirements, with an advanced ethylene production process using a SiC tube heat exchanger, are projected at 63.9 trillion Btu per year.

Selective Inorganic Thin Films

Tina M. Nenoff, Steven G. Thoma, Daniel Trudell,
Diana Fisler, Alejandra Chavez, and Phillip I. Pohl
Sandia National Laboratories
Albuquerque, NM 87185

INTRODUCTION

Separating light gases using membranes is a technology area for which there exist opportunities for significant energy savings. Examples of industrial needs for gas separation include hydrogen recovery, natural gas purification, and dehydration. A membrane capable of separating H_2 from other gases at high temperatures could recover hydrogen from refinery waste streams, and facilitate catalytic dehydrogenation and the water gas shift ($CO + H_2O \rightarrow H_2 + CO_2$) reaction. Natural gas purification requires separating CH_4 from mixtures with CO_2, H_2S, H_2O, and higher alkanes. A dehydrating membrane would remove water vapor from gas streams in which water is a by-product or a contaminant, such as in refrigeration systems.

Molecular sieve films offer the possibility of performing separations involving hydrogen, natural gas constituents, and water vapor at elevated temperatures with very high separation factors. It is in applications such as these that we expect inorganic molecular sieve membranes to compete most effectively with current gas-separation technologies. Cryogenic separations are very energy intensive. Polymer membranes do not have the thermal stability appropriate for high-temperature hydrogen recovery, and they tend to swell in the presence of hydrocarbon natural gas constituents. Our goal is to develop a family of microporous oxide films that offer permeability and selectivity exceeding those of polymer membranes, allowing gas membranes to compete with cryogenic and adsorption technologies for large-scale gas-separation applications.

TECHNICAL PROGRESS

We have a CRADA in effect to develop inorganic thin-film membranes for the separation of a tonnage commodity hydrocarbon chemical feedstock. Our CRADA team consisted of the Amoco Chemical Company and Sandia National Laboratories. This CRADA went into effect June 1997. During FY 1998, we successfully built a team consisting of Amoco, Coors Technical Ceramics Company, and Sandia and submitted a proposal to the Vision 2020: The Chemical Industry, entitled “Advanced Materials for Reducing Energy Consumption and Manufacturing Costs in the Chemicals and Petroleum Refining Industries.” We were awarded the grant toward the end of FY 1998. The committed combined in-kind cost share for this from the industrial partners is 56% for this 3-year program. Success in this program will result in the following:

- Extreme energy savings of about 105 trillion Btu per year by the year 2020 for the U.S. chemical industry.
- Reduced capital expenditure in the chemical industry.

- Great reduction in the nation's dependence on imported fossil fuel.

ENERGY SAVINGS/WASTE REDUCTION

Amoco's Chemical sector is the world's largest manufacturer of various industrially important feedstock chemicals. The production of the one feedstock in focus is energy intensive, relying either on adsorption or cryogenic processing for purification. ***Last year, nearly 7 billion pounds of the hydrocarbon were produced in the United States at an estimated energy requirement of 28 trillion Btu.***

While there have been incremental improvements to the critical separation processes used by the chemicals and petroleum refining industries, there have been no significant breakthroughs. Conventional distillation, adsorption, and crystallization technologies are still being used to isolate and purify products.

Sandia, Amoco, and Coors Ceramics will cooperate in this project to develop membranes that effectively separate one isomer of the feedstock from the natural mixture of isomers. The key technical hurdle in the development of this novel separation concept is the precise control of the pore structure and adsorption properties of the membrane materials. The advantages offered by zeolite composite membranes are uniform pore size distribution, shape selectivity based on tailored pore size, chemical and mechanical stability, and high-temperature stability.

A technology breakthrough in separation processing is crucial to the U.S. hydrocarbon industry, as it would result in yearly energy savings of **about 105 trillion Btu by the year 2020**. Improved hydrocarbon gas–separation processes will reduce U.S. energy requirements and dependence on oil imports. This key separation area is currently conducted primarily by cryogenic distillation; extremely low temperatures (–90°C) and corresponding high refrigeration costs and high compressor utility charges characterize this process. It is estimated that a 1-billion-per-year commercial plant that uses this cryogenic crystallization process would consume 4 ***trillion Btu*** of energy. Based on annual production figures, this translated to energy consumption of ***24 trillion Btu*** for this hydrocarbon isomer's separations alone. Energy-efficient separation processes involving novel microporous inorganic thin-film materials can lead to significant energy savings compared to conventional adsorption or cryogenic processes. ***The end effect would be about 75% energy reduction in production and about 60% capital reduction.***

MODELING

Initially, modeling screened pore dimensions by simulating permeation of single gas molecules through the best four zeolite pores in terms of high selectivity and permeability. This conclusion was made excluding entrance effects. In the next round of computations, Fig. 1, these four zeolite phases were tested for hydrocarbon permeation, including the entrance effect. In this case, one zeolite clearly outdistanced itself from the others, again in terms of higher selectivity and permeability.

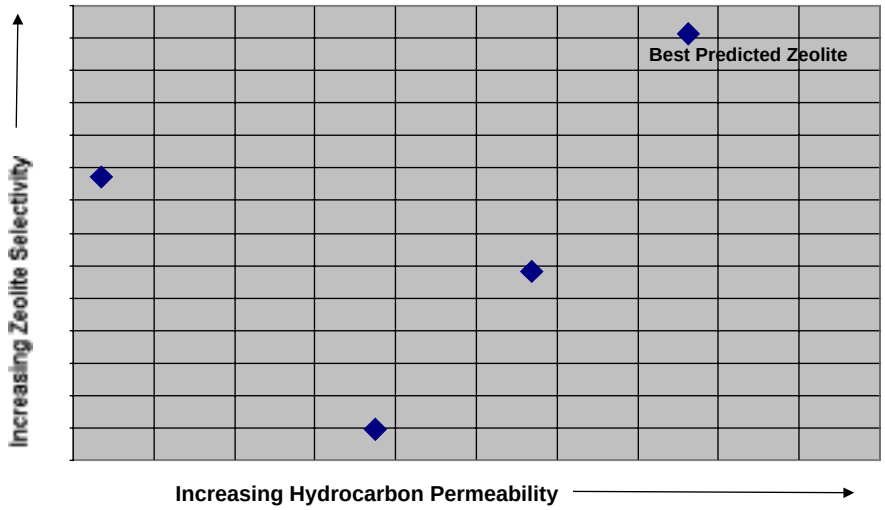

Fig. 1. Zeolite performance (450K).

The simulation portion of this project has continued to focus on the transition-state energy barriers to adsorption and permeation of various isomers. In particular, the isovalent substitution of various tetrahedral cations into the "best" framework structure has been explored in more detail because of the reduced adsorption energy for certain isomers with respect to neutral frameworks (Fig. 2). This "best" structure is being evaluated to determine the effect of acid sites in addition to purely steric changes in the structure. Molecular dynamics simulations using LAMMPS (Large-scale Atomic/Molecular Massively Parallel Simulator, a MD code by S. Plimpton) are being prepared to begin to evaluate the effect of increasing gas concentrations.

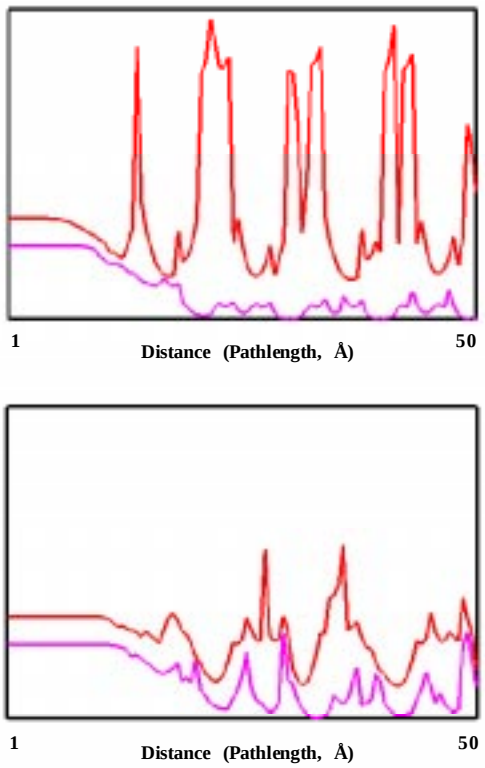

Fig. 2. Interaction energies of similar hydrocarbons permeating through an all-silica (top) and a metal-doped (bottom) silica zeolite membrane.

Synthesis

Concurrent to the modeling effort for predicting separations through inorganic crystalline pores, we have been synthesizing various membranes in the lab. We have focused on the best zeolite structure, due to results presented in the modeling, while studying such variables as composition, crystallite size, extent of coverage, supports, and "caulking" media. Each membrane synthesized is characterized also by X-ray diffraction, SEM (top and cross-sectional views), and EDS for phase identification and integrity. Permeation studies with various-sized gas and organic molecules and the synthesis of the zeolite structures with elemental dopants are under way.

The sequence of deposition of components in the film has been the focus of our recent efforts. The zeolite phase is synthesized as a membrane on the substrate with an organic structure-directing agent that resides in the pores of the phase. We have been able to synthesize this phase with a high degree of crystal orientation; the pores of the crystallites are parallel to the flow direction (see Fig. 3). (This procedure has been submitted as a patent technical advance to Sandia National Laboratories.) A calcination step is then necessary to remove the occluded organic molecule, so that the pathway for permeating molecules will be opened. With different synthesis procedures, followed by calcination, a defect-free composite thin film composed of amorphous and crystalline zeolite phases is produced (see Fig. 4). The result is an approximate 10× increase in selectivity of He over SF_6 (our test molecules for defect sites).

Before calcination, the Defect-Free membrane does not allow permeation of N_2 or SF_6.

After calcination:

$$N_2 = \mathbf{1.7 \times 10^{-2}}\ \text{cc(STP)/cm}^2\text{/s/cmHg at 30°C}$$
$$N_2/SF_6 = \mathbf{1.8},\ <\text{Knudsen } N_2/SF_6 \ \underline{a}\ 2.3 \text{ (ideal)}$$

Composite Membrane (post calcination; amorphous/zeolite film)

$$N_2 = \mathbf{2.7 \times 10^{-3}}\ \text{cc(STP)/cm}^2\text{/s/cmHg at 30°C}$$
$$N_2/SF_6 = \mathbf{9.8}$$

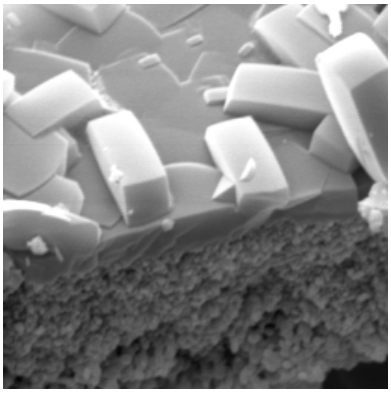

Fig. 3. Highly oriented crystalline Zeolite thin film (cross-sectional view).

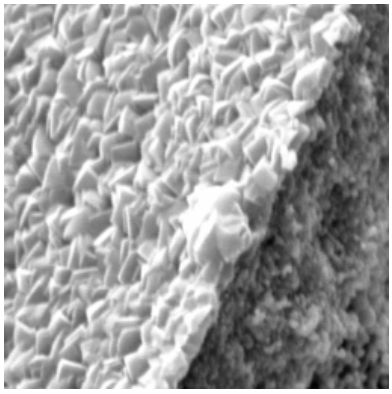

Fig. 4. Zeolite/Sol-gel composite film on alumina substrate (cross-sectional view).

Permeation Studies

A compact membrane test unit has been designed and built to collect permeation and separation selectivity data on various prepared and synthesized materials. The unit readily fits into a 1.6-ft^3 convection oven. The unit is assembled from commercially available Swagelok® and Cajon® Ultra-Torr tube fittings. The unit can be operated at temperatures up to 200°C and pressures to 150 psig. A Hewlett Packard gas chromatograph with a combination flame-ionization detector (FID)/unit resolution quadrupole mass spectrometer provide analytical capabilities for the unit.

A list of associated equipment and materials used to conduct permeation studies follows:

- 1.6-ft^3 oven with programmable temperature control from 30 to 200°C.
- Brooks mass-flow controllers and power-supply readout.
- Tylan back-pressure regulator.
- Hewlett Packard 5890 Series II gas chromatograph with FID and wide bore-capillary columns.
- Hewlett Packard 5791 Mass Selective Detector with jet separator.
- He, N_2, SF_6, butane, isobutane, and various hydrocarbon and hydrocarbon/inert gas blends.
- Dual-Stage gas regulators for respective gases and gas manifold for flow, addition, and mixing of gases.

SUMMARY

The molecular sieve membranes described in this report consist of films of microporous phases deposited on porous supports. The films must cover the substrate completely in order to demonstrate any selectivity based on molecular sieving, and the films must be thermally durable enough to withstand operating temperatures and/or calcination. In particular, the film must survive the thermal-expansion mismatch between itself and the substrate without cracking or peeling. In our membranes this is accomplished by incorporating an amorphous phase that acts as a binder or "caulk." The limited porosity of the amorphous phase reduces nonselective gas flow between zeolite crystals, while its flexibility mitigates the thermal-expansion mismatch between the film and the substrate.

Started in FY 1997 and continuing through September 1999, the following milestones will be met for the CRADA:

A. Model the permeation of hydrocarbon mixtures through zeolite structures in order to identify the crystalline phase that will maximize permeability of specific hydrocarbon molecules in an equilibrium vapor stream.

B. Synthesize leak-free composite membranes by caulking zeolite films with sol-gels.

C. Test permeation of various light gases and organic hydrocarbon molecules at various temperatures, pressures, and mixture ratios.

IMPACT

Molecular sieving membranes of this type are capable of separating a number of chemical and refining mixtures. Substantial energy savings (as much as 75%) will be realized by replacing current energy-intensive cryogenic or adsorption separations with membrane-separation technology.

PUBLICATIONS

T. M. Nenoff, A. V. Chavez, S. G. Thoma, W. T. A. Harrison, and M. L. F. Phillips, "Organically Templated Zinc Phosphate Phases," *MRS Symposium Series* 497 (1998).

W. T. A. Harrison and M. L. F. Phillips, "Crystal Structures of Novel Guanidinium Zinc Phosphates," *Chem. Mater.* **9**, 1837 (1997).

A. Martino, S. A. Yamanaka, J. S. Kawola, and D. A. Loy, "Encapsulation of Gold Nanoclusters in Silica Materials via an Inverse Micelle / Sol-Gel Synthesis," *Chem. Mater.* **9**(2), 423 (1997).

B. G. Karle, C. J. Brinker, and M. L. F. Phillips, "Zeolite Membranes from Kaolin," *Mat. Res. Soc. Symp. Proc*. **431**, 1997 (in press).

W. T. A. Harrison and M. L. F. Phillips, "Template Cooperation Effect Leading to 18-Ring Cavities in the Open-Framework Guanidine Zincophosphate $(CN_3H_6)_3 \bullet Zn_7(H_2O)_4(PO_4)_6 \bullet H_3O$," *Chem. Comm.* 2771–72 (1996).

PRESENTATIONS

T. M. Nenoff, S. G. Thoma, C. Ashley, and S. Reed, "Defect-Free Molecular Sieve Membranes," Fall National ACS meeting, Boston, Massachusetts, August 1998.

D. Fisler, P. I. Pohl, and T. M. Nenoff, "Simulation of Pore diffusion and adsorption in Zeolites," Fall National ACS meeting, Boston, Massachusetts, August 1998.

T. M. Nenoff, A. V. Chavez, S. G. Thoma, P. Provencio, W. T. A. Harrison, and M. L. F. Phillips, "Amine Templated Zinc Phosphate Phases for Membrane Separations," Spring National MRS meeting, San Francisco, California, April 1998.

D. Fisler, P. I. Pohl, and T. M. Nenoff, "Modeling of Gas Permeation in Zeolite Membranes," Spring National MRS meeting, San Francisco, California, April 1998.

T. M. Nenoff and M. Ali, "Selective Inorganic Thin Films," AIM Program Annual Review, Jackson, Wyoming, June 23–25, 1998.

SYMPOSIUM ORGANIZED

A symposium entitled "Catalysis with Designed Materials" was accepted by the Colloid and Surface Science Division of the American Chemical Society, and was held at the Fall

1998 Boston National ACS Meeting. Tina Nenoff, the organizer, was able to raise $10K in speakers' funds from various ACS departments and industrial sponsors. (Approximately 50% of the participants were from industry.) The focus of the symposium included the use of computer modeling, tied with materials synthesis, to efficiently predict and synthesize novel materials for catalysis and separations. The work from this AIM program, particularly from the CRADA, was presented at the symposium.

PATENTS

None.

PATENT DISCLOSURES

S. G. Thoma and T. M. Nenoff, "A New Method of Synthesizing Highly Oriented, Zeolite Crystalline Thin Film Membranes," SD-6216.

S. G. Thoma, T. M. Nenoff, C. Ashley, and S. Reed, "A New Mehtod for Synthesizing Defect-Free Thin Film Membranes: Composite Zeolite/Sol-Gel Membranes," SD-6222.

M. Phillips, "A Thermally Stable Zinc Phosphate Molecular Sieve," SD-5962.

M. Phillips, "A New Method for Preparing Zinc Oxide Thin Films from Solution," SD-5963.

LICENSES

None.

INDUSTRIAL INPUT AND TECHNOLOGY TRANSFER

As part of the Vision 2020 grant and the CRADA, Amoco Chemical Co. will provide hydrocarbon-separations testing on lab-bench and pilot plant–scale apparatus. Amoco also will determine economic and chemical feasibility of scaleup to a pilot plant. Coors Technical Ceramics Company will study the scaleup and production of the developed membranes.

Cost Sharing

The 3-year, $2.769M CRADA has been signed and is in effect between Sandia National Laboratories and the Amoco Chemical Company. Amoco is to contribute in-kind funds in the following manner: $512K for year 1; $480 for year 2; $502 for year 3. The start date was June 16, 1997.

As of September 1998, our CRADA team has been awarded a 3-year, $4.295M Vision 2020: The Chemical Industry grant. The team has expanded to include Sandia National Laboratories, Amoco Chemical Company, and Coors Technical Ceramics Company. Amoco is to contribute in-kind funds in the following manner: $700K for year 1, $700K for year 2, and $700K for year 3; Coors is to contribute in-kind funds in the following

manner: $50K for year 1, $100K for year 2, $150K for year 3. This combines to a 56% in-kind funding from industrial partners.

HIGHLIGHTS

We began a CRADA (June 1997) with Amoco Chemical Co. to study the feasibility of using shape-selective molecular sieve membranes to enrich hydrocarbon feedstocks from mixtures of the isomers. In FY 1998, we were awarded a 3-year, $4.295M Vision 2020: The Chemical Industry grant, which will support the CRADA with the expanded team of Sandia National Laboratories, Amoco Chemical Company, and Coors Technical Ceramics Company. We are continuing to synthesize shape-selective composite zeolite/sol-gel membranes using crystalline phases identified by molecular modeling for hydrocarbon separations. Permeation studies are ongoing at both Sandia and Amoco with these Sandia-synthesized membranes.

Project Investigators

In FY 1998 this project involved the following participants from Sandia National Laboratories, Albuquerque, New Mexico (SNL); University of New Mexico, Albuquerque, New Mexico (UNM); and the University of Western Australia, Nedlands, Washington (UWA).

NAME	Project Role
Dr. Tina M. Nenoff, SNL	Principal investigator, film synthesis
Dr. Diana Fisler, SNL	Permeation modeling
Dr. Phillip I. Pohl, SNL	Permeation modeling
Dr. Anthony Martino, SNL	Nanocluster catalysts
Alejandra V. Chavez, SNL & UNM	Molecular sieve synthesis
Steven G. Thoma, SNL	Membrane synthesis
Daniel Trudell, SNL	Permeation unit construction, testing
Prof. William T. A. Harrison, UWA	Crystallography

Polymers

Polymer Electrolyte Electrochemical Reactors of Lowered Energy Consumption

S. Gottesfeld
Electronic and Electrochemical Materials and Devices, MST-11
Los Alamos National Laboratory
Los Alamos, New Mexico 87545

The Conducting Polymer project funded by the AIM Program has developed new methods for the synthesis of conducting polymers and evaluated new industrial applications for these materials that would result in significant reductions in energy usage or industrial waste. Along these lines, we continued to research and develop during 1998 electrochemical reactors (ECRs) based on polymeric electrolytes. In the chlor-alkali industry, electrochemical reactors based on polymer electrolyte membranes consume around 2% of the total electric power generated in the United States. Our ECR R&D activity, which started in FY 1996, is devoted to major energy savings in this industry. Energy savings as high as 50% could be achieved with the advanced ECR technology being developed by us. Corresponding, highly significant lowering in CO_2 emissions would result.

BACKGROUND

During FY 1998, we continued to explore a scheme and effective cell design for significantly reducing energy consumption in a chlor-alkali ECR, using an oxygen cathode and a cation-conducting polymeric membrane (CCM). Figure 1 shows the basic idea of the advanced, polymer membrane–based ECR that we now develop. The conventional configuration of a chlor-alkali ECR that generates chlorine and caustic soda by electrolysis of sodium chloride brine, is shown on the left-hand side of Fig. 1. The cell voltage required for significant electrolysis rates of 300 A/ft^2 is 3.2 to 3.3 V. Energy consumption per unit weight of the products (chlorine and sodium hydroxide) is directly proportional to cell voltage. Lowering cell voltage at given current density (i.e., at given production rate) is therefore the key for achieving energy savings in this industrial process that consumes 2% of the electric energy produced in the United States.

It has been recognized some time ago, that, if the hydrogen-evolving cathode were replaced by an oxygen-reducing cathode, the voltage of the cell could be reduced, in principle, by about 0.9 V. The change of the cathodic process by introduction of oxygen as cathode reactant and the corresponding expected lowering in cell voltage are schematically depicted on the right hand side of Fig. 1. To achieve the expected savings in cell voltage from introduction of oxygen as “cathode depolarizer,” a very effective oxygen electrode is required. Furthermore, the cell configuration has to be such that a gas-supplied (oxygen) cathode could operate side-by-side with a liquid-filled (brine) adjacent cell compartment. Neither of these targets has been easy to achieve, and the result has been that the concept of a chlor-alkali cell with an oxygen cathode has not yet been implemented commercially. This is in spite of the fact that efforts to prove

feasibility of the concept continue to date, particularly in Japan where the availability and cost of electric power are more significant issues today than in the United States.

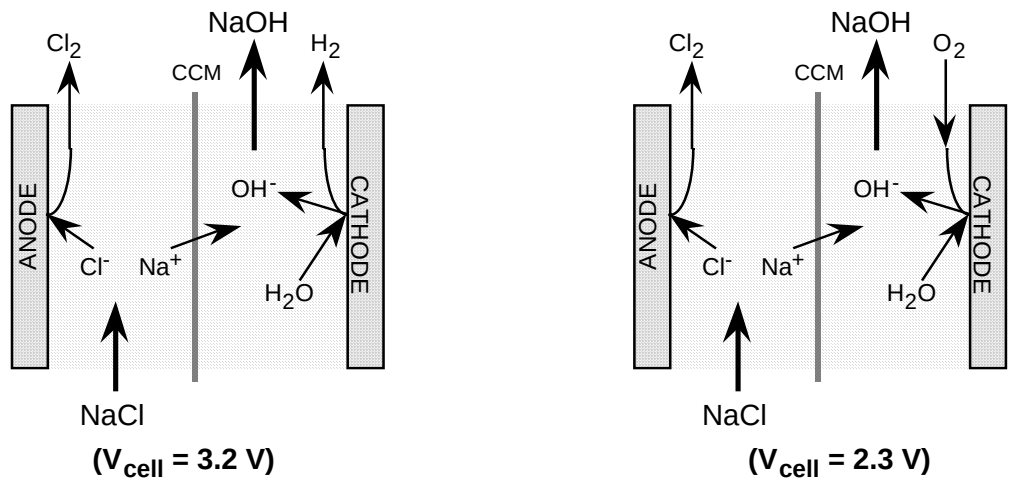

(a) Conventional Chlor-Alkali Cell

(b) Chlor-Alkali Cell with Oxygen Cathode

Fig. 1: Scheme for reducing energy consumption in a chlor-alkali ECR, using an effective oxygen cathode and a cation conducting polymeric membrane (CCM) as basis for an effective membrane/electrode assembly. The cell voltages shown correspond to a cell current density of 300A/ft^2 in each case.

** With stronger attention to the generation rate of CO_2 in the context of global warming concerns, possible cutting of 50% of the total volume of CO_2 generated by this major U.S. industry may become a significant target.**

In light of the energy-savings incentives described above, we have adapted in 1996 an advanced oxygen electrode technology, developed at LANL originally for application in polymer electrolyte fuel cells, for application in chlor-alkali ECRs. An important element of the new project has been immediate industrial interest: Dow Chemical expressed interest in working with us on this project based on a Cooperative Research and Development Agreement (CRADA).

TECHNICAL PROGRESS: FY1998

Implementation of Dow Test Hardware and Modification of Oxygen Cathode for Use in It

Adaptation by LANL of a small-scale reactor (58 cm^2), employed for testing and development in the Dow chlor-alkali laboratory at Freeport, Texas, was implemented near the end of FY 1997. Selection of this cell type was originally made to compare directly with the performance obtained by Dow in an exact same cell configuration under ordinary mode of chlor-alkali ECR operation (with hydrogen-evolving cathode). In addition, successful implementation of the LANL oxygen cathode in a Dow-type cell

structure could have allowed, at least in principle, simple retrofitting of existing industrial cells. Such retrofitting would involve a change limited to replacement of the cathode only, while maintaining the rest of the current cell components and hardware.

A new system at LANL has been designed and built to accommodate continuous operation of three larger test cells in parallel. Several engineering controls were designed and implemented to maintain desired solution concentrations, including a chlorine scrubber system to safely convert chlorine gas to ordinary “bleach” for disposal and a brine-purification system. Brine purification was given up later in 1998 in favor of “importing” highly pure brine from the Freeport, Texas, plant of Dow Chemical. The reason was that a significant level of colloidal silicates in the Los Alamos water system could not be removed either by ion exchange or by any other purification technique. The brine now arrives regularly from Freeport in plastic drums, eliminating any need for local purification.

The low pressure across the industrial cell components (about 1 psi) was one feature of the Dow cell that seemed to present additional barriers to achieving high cell performance on introduction of the LANL oxygen cathode. However, having understood the important engineering advantages of cell retrofitting, we continued to experiment for much of 1998 with the original Dow test cell structure, targeting low and stable overall cell resistances. By going through several iterations of cathode structures, quite good performances (e.g., cell voltage of 2.3 V at 350 A/ft^2) were observed initially, but subsequently the performance degraded (i.e., the cell voltage continuously increased at given constant current). Often the cell resistances observed reached 3 Ω cm^2 and were the main reason for the high overall cell voltage (a typical value for ECRs based on such bilayer, cation-conducting membranes is 1.5 Ω cm^2).

Figure 2 demonstrates the typical problem observed with a Dow-type test cell, operating with a LANL oxygen electrode. In the test depicted, the throughput of the cell was doubled vs the ordinary chlor-alkali throughput, while maintaining the voltage initially below the voltage of the state-of-the-art chlor-alkali ECR (3.0 V vs 3.2 V). However, as time progressed, the resistance of the cell kept creeping up, generating a creep-up of cell voltage. It was this type of apparent instability in cell performance, associated with resistance and, hence, voltage creep-up, that brought us to decide, after the AIM program review in Jackson Hole, to rethink the cell design in an attempt to achieve a lower and more stable cell resistance.

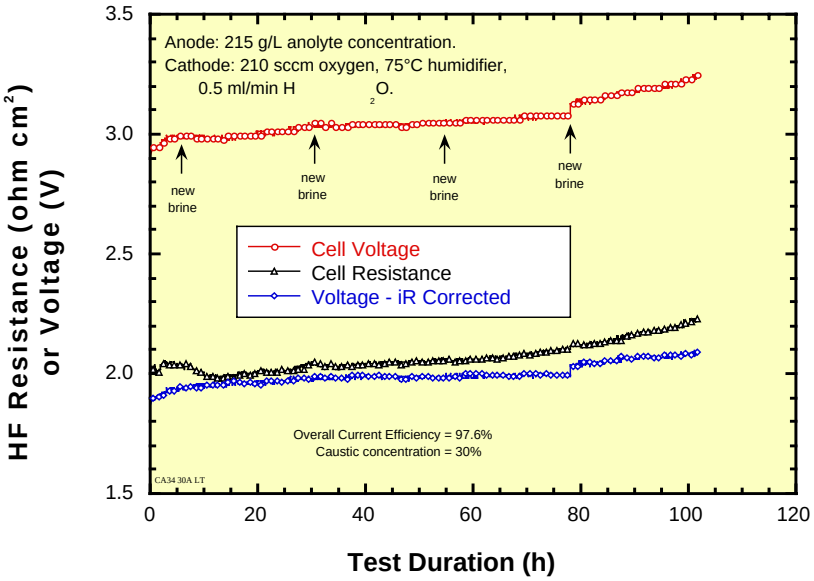

Fig. 2. Cell polarization (upper curve), iR-corrected polarization (bottom curve), and cell resistance (middle curve) as function of time in a life test of a modified Dow-type test cell with an oxygen electrode, operating at enhanced current density of 600A/ft^2 (twice the ordinary chlor-alkali current density).

Breakthrough Achieved with New Cell Design Introduced During Second Half of FY 1998

Significant improvements in cell performance and performance stability

Note: Because of CRADA protection issues and a pending patent application, details of the configuration of the most recent oxygen depolarized chlor-alkali ECR, developed and demonstrated during the second half of FY 1998, will not be given here. Only results of testing will be described.

Following evaluation of possible reasons for the high and continuously increasing cell resistance in our tests with the Dow cell hardware during the first half of 1998, LANL and Dow Chemical jointly decided on exploring another cell configuration. This turned out very successfully. Tests with the new configuration implemented by LANL were first performed in September of 1998, covering a range of cell currents from ordinary chlor-alkali cell current densities to almost three times higher. The cell resistances measured were now significantly lower, for example, 1.2 ohm cm^2 measured for a cell operating at 0.4 A/cm^2, and, most important, they remained stable over a period of 100 h and more of continuous operation. As a result, the following stable cell performance points were recorded: cell voltage of 2.2 V at 400 A/ft^2, 2.45 V at 600 A/ft^2, and 2.7 V at 800 A/ft^2.

Note that the latter result means a chlor-alkali ECR that achieves an increase in throughput from same size cell (and probably same cost) by a factor of 2.5 vs that achievable with the current ECR technology, and, at the same time, still cuts electric energy input per ton of chlorine product by 16%. Alternatively, maintaining the

throughput per given cell size would enable achievement of the full expected savings in energy associated with a cut by a full 1.0 V out of 3.2 V (i.e., 31% cut in electric energy input per unit chlorine product). Having already demonstrated the potential of this technology to enable trade-off between plant size/cost and electric energy invested per ton of product, a specific choice can/will be made based on local circumstances.

We strongly believe that the most recent results demonstrated by us, with a new structure of chlor-alkali ECR employing an oxygen cathode, are unique. We are not aware of any comparable achievement in terms of the ECR structure, the high energy savings, and the possibility of much higher throughput per cell size, while still maintaining a significant fraction of the energy savings. We are pursuing vigorously a patent application and have seen significant interest from our industrial partner in the IP evolving from this work.

Industrial input and technology transfer: Collaboration with Dow Chemical and CRADA

A CRADA between UC (LANL) and Dow Chemical was executed first on June 18, 1997, to include the collaborative effort on chlor-alkali ECRs of lowered electrical energy consumption. The LANL effort in this collaboration has been the continuation of our project under the AIM program on ECRs of Lowered Energy Consumption.

The JWS includes materials, components, and cell-configuration optimization efforts to be pursued at LANL, the techno-economic evaluation of the merit of this concept as a function of plant location that affects cost of power and marketability of hydrogen, and the pilot plant testing to be performed in the third year of the project to the degree justified by preceding life tests in smaller cells. We are employing materials and cell structure optimized by LANL work during the first 2 years.

We had excellent opportunities during FY 1998 to continue to interact with Dow Chemical. They visited Los Alamos several times during this year, and we have visited twice their central chlorine production facility and established contact with production engineers. We have had ample opportunity during these visits to discuss in depth a strategy for demonstration of the concept at pilot plant level.

Industrial input and technology transfer; expansion of effort: CRADA under OIT (chemical industry)

With encouragement and advice from Charles Sorrell of the AIM program office, we pursued at the beginning of 1998 an expansion of this R&D project, by dividing it into a stronger cell-testing and ECR technology-transfer element, while further pursuing a materials- and process-optimization component. The former element has been strengthened within the CRADA with Dow Chemical and also supported from the OIT/Chemical Industry office (Amy Manheim is the program manager at DOE/HQ).

Note: As this report is written (early 1999), arrangements are being made to start experimenting at the Dow plant in Freeport in the spring of 1999 with the newest ECR cell design demonstrated at LANL late in 1998; at this time, we plan to confine testing to the lab cell sizes tested at LANL (50-cm^2 active area).

In parallel, the continued requirements of developing new materials and configurations for the unique ECR configuration demonstrated most recently call for extensive studies of the mechanical and electrochemical characteristics of materials (and specific structures), including particularly corrosion susceptibility. The oxygen cathode requires moving away from the materials and flow field employed in initial ECR demonstration to materials and structures that will provide satisfactory mechanical properties in actual cell dimensions of several feet in height and width. The natural choice of metallic components, from a mechanical perspective, will have to be followed by judicious choice of metal components with or without surface treatment that can withstand the caustic environment and the potential of an oxygen cathode. The latter is a very important difference vs the state-of-the-art chlor-alkali cell, which uses hydrogen cathodes, because the cathode potential in the latter case provides better cathodic protection. All of those materials issues, highly unique to this specific cell and application, will continue to be pursued under the AIM program.

HIGHLIGHTS

A new cell configuration, introduced by us in the fall of 1998, turned out to be very successful in providing high performance and performance stability of a chlor-alkali ECR employing an oxygen cathode, as a result of significant lowering of cell resistance and the ability to stabilize such low resistance in long-term (hundreds of hours) operation. Tests with the new configuration implemented were first performed in September of 1998; they cover a range of cell currents, from ordinary chlor-alkali cell-current densities to some almost three times higher. The cell resistances measured were now significantly lower, for example, 1.2 ohm cm^2 measured for a cell operating at 0.4 A/cm^2, and, most important, they remained stable over a period of 100 h and more of continuous operation. As a result, the following stable cell performance points were recorded: cell voltage of 2.2 V at 400 A/ft^2, 2.45 V at 600 A/ft^2, and 2.7 V at 800 A/ft^2. This is to be compared with state-of-the-art ECRs in the chlor-alkali industry, which operate at 3.2 V at current density of 300 to 400 A/ft^2. Note that maintaining the throughput per given cell size achieves the full expected savings in energy associated with a cut by a full 1.0 V out of 3.2 V (i.e., 31% cut in electric energy input per unit chlorine product). On the other hand, operating at 800 A/ft^2 / 2.7 V means a chlor-alkali ECR that achieves an increase in throughput from the same size cell by a factor 2.5 vs the present ECR technology and, at the same time, still cuts electric energy input per ton of chlorine product by 16%.

We strongly believe that the most recent results demonstrated by us with the new chlor-alkali ECR based on an oxygen cathode are very unique. We are not aware of any comparable achievement in terms of unique ECR structure, the high energy savings, and the possibility of much higher throughput per cell size while still maintaining a significant fraction of the energy savings. We are pursuing vigorously patent application.

With encouragement and advice from Charles Sorrell of the AIM program office, we pursued at the beginning of 1998 an expansion of this R&D project, enhancing the cell-testing and tech-transfer element while pursuing in parallel materials-optimization issues. The former element has been strengthened now within a CRADA with Dow Chemical, further supported with funding from the OIT/Chemical Industry office. *Note: As this*

report is written (early 1999), arrangements are being made to start experimenting at the Dow plant in Freeport in the spring of 1999, with the newest ECR cell design demonstrated at LANL late in 1998; for the moment, testing will be confined to the lab cell sizes tested at LANL (50-cm^2 active area).

PROJECT INVESTIGATORS

Name	Activities	FTE
Gottesfeld	Principal Investigator Planning and Supervision	0.25
Christine Zawodzinski	Reactor fabrication and testing	0.50
Mahlon Wilson	Reactor Design and Testing	0.30
Chuck Derouin	Technical Assistance	0.20
Don McMurray	Technical Assistance	0.15

Internal Distribution

1–2. Central Research Library
3. Document Reference Section
4–5. Laboratory Records Department
6. Laboratory Records, ORNL RC
7. ORNL Patent Section
8. P. Angelini
9. B. R. Appleton
10. G. A. Aramayo
11. S. Babu
12. R. L. Beatty
13. T. M. Besmann
14. E. E. Bloom
15. C. A. Blue
16. P. A. Boyd
17. R. A. Bradley
18. K. Breder
19. C. R. Brinkman
20. G. M. Caton
21. R. H. Cooper, Jr.
22. D. F. Craig
23. S. A. David
24. R. B. Dinwiddie, Jr.
25. G. M. Goodwin
27. H. W. Hayden, Jr.
28. L. L. Horton
29. C. R. Hubbard
30. T. J. Huxford
31. D. R. Johnson
32. R. R. Judkins
33. M. A. Karnitz
34. J. R. Keiser
35. C. T. Liu
36. K. C. Liu
37. Gail M. Ludtka
38. P. J. Maziasz
39. A. E. Pasto
40. S. J. Pawel
41. B. A. Pint
42. M. L. Santella
43. A. C. Schaffhauser
44. V. K. Sikka
45. P. S. Sklad
46. R. W. Swindeman
47. S. Viswanathan
48. X. L. Wang
49. A. Wereszczak
50. J. M. Wyrick
51. T. Zacharia

External Distribution

52. ABB-CE Power Products Manufacturing, Combustion Engineering, Inc., 1119 Riverfront Parkway, Chattanooga, TN 37402
    Jeff Henry

53. ABB-Combustion Engineering, Inc., 911 West Main Street, Chattanooga, TN 37402
    Domenic Canonico

54–56. ABB-Combustion Engineering, Inc., 200 Great Pond Dr., P.O. Box 568, Windsor, CT 06095-0568
    Hank Arenstam
    Reddy Ganta
    Mark LeBel

57. ABB-Combustion Engineering, Inc., 200 Day Hill Road, P.O. Box 500, Windsor, CT 06095
    Thomas Gibbons

58–59. ACuPowder International, LLC, 901 Lehigh Avenue, Union, NJ 07083
    Edul M. Daver
    Krishna Patel

60. Acutus Gladwin, Airport Office Park, Bldg. 1, 410 Rouser Rd., 5th Floor, Corapolis, PA 15108
    James B. Sears, Jr.

61. Advanced Refractory Technologies, Incorporated, 699 Hertel Avenue, Buffalo, NY 14207
    Keith A. Blakely

62–63. Ahlstrom Recovery, Incorporated, 10745 Westside Parkway, Alpharetta, GA 30004
    James P. Martin
    Jorma Simonen

64. AHT, Inc., 1024 Kittanning Pike, P.O. Box U, Chicora, PA 16025-0491
    Gary Hudson

65. Alabama Pine Pulp Company, Inc., P.O. Box 100, Perdue Hill, AL 36470
    Sunil Chandnani

66. ALCOA, 100 Technical Drive, Aloca Center, PA 15069-0001
    Thomas Meyer

67. Alcon Industries, Inc., 7990 Baker Avenue, Cleveland, OH 44102
William Habansky

68–69. Alfred University, Center for Advanced Ceramic Technology, Alfred, NY 14802
Richard M. Spriggs
Harrie J. Stevens

70. Alfred University/NYSCC, Alfred, NY 14802
Doug Korwin

71. Allied-Signal Aerospace Company, Garrett Ceramic Components Division, 19800 S. VanNess Avenue, Torrance, CA 90509
Maxine L. Savitz

72. Allied-Signal, Incorporated, Ceramics Program, P.O. Box 1021R, Morristown, NJ 07960
Clifford P. Ballard

73–74. Alloy Engineering and Casting Company, 1700 West Washington Street, Champaign, IL 61821
James R. Lytle
David Robinson

75. Alstrom Machinery, Incorporated, 10745 Westside Parkway, Alpharetta, GA 39201
Peter Collins

76. American Axle and Mfg., 1840 Holbrook Avenue, Detroit, MI 48212-3488
Michael E. Stevens

77. American Forest & Paper Association, 1111 19th Street, NW, Suite 800, Washington, DC 20036
David Cooper

78. Ames Laboratory, Iowa State University, 126 Metals Development, Ames, IA 50011-3020
Iver Anderson

79. Ames Laboratory, Iowa State University, 204 Metals Development, Ames, IA 50011-3020
D. C. Jiles

80. Ames Laboratory, Iowa State University, 137 Wilhelm, Ames, IA 50011-3020

Tamara Bloomer

81–85. Ames Laboratory, Iowa State University, 214 Wilhelm, Ames, IA 50011-3020

L. S. Chumbley
H. Mahmood
K. L. Pauwels
P. P. Pulvirenti
R. Bruce Thompson

86. Ametek, Specialty Metals Products Division, Rt 519, P.O. Box 427, Eighty Four, PA 15330

John H. Reinshagen

87–89. Amoco, 150 West Warrenville Road, Naperville, IL 60563-8460

Moin Ali
Martin Carrera
Charles Scouten

90–91. Anchor Glass Container, One Anchor Plaza, MP 27, 4343 Anchor Plaza Parkway, Tampa, FL 33634-7513

Michael Nowson
Samuel Wilson

92. AP Green Industries, 1 Green Blvd., Mexico, MO 65265

John Conrad

93. Argonne National Laboratory, 9700 South Cass Avenue, Argonne, IL 60439

Bob Dunlap

94–95. Babcock & Wilcox, 2302 Parklake Drive, NE, Suite 300, Atlanta, GA 30345

Robert Larsen
Thomas F. Roberts

96. Babcock & Wilcox, 90 East Tuscarawas Avenue, Barberton, OH 44203-0665

Gregory M. Pifer

97–98. Babcock & Wilcox, 20 S. Van Buren Avenue, P.O. Box 351, Barberton, OH 44203-0351

Joan Barna
J. William Smith

99. Ball-Foster Glass Container Co., PO Box 4200, Muncie, IN 47307

Marv Gridley

100. Battelle, 505 King Avenue, Columbus, OH 43201-2693

Jeffrey Colwell

101–102. Battelle Pacific Northwest Laboratories, Department of Materials Science, P.O.Box 999, Richland, WA 99352

Gregory J. Exarhos, K2-44
Gary L. McVay, K2-45

103–104. Bethlehem Steel Corporation, P.O. Box 248, Chesterton, IN 46304

Dan Elwood
Anthony Simola

105–106. Black & Decker, Incorporated, 701 East Joppa Road, TW 460, Towson, MD 21286

Nick Achterberg
Stephen R. Crosby

107–108. The Carborundum Company, P.O. Box 187, Keasbey, NJ 08832

Craig L. Dillman
Stanley Gursky

109. Carpenter Technology Corporation, 92 Burning Tree Lane, Reading, PA 19607

Robert L. Caton

110–111. Carpenter Technology Corporation, 101 West Bern Street, P.O. Box 14662, Reading, PA 19612-4662

Bradford A. Dulmaine
Nicholas Fiore

112–113. Caterpillar Incorporated, Building E, P.O. Box 1875, Peoria, IL 61656-1875

Michael H. Haselkorn
Kaichu Hsieh

114. Caterpillar Incorporated, 3701 State Road, 26 East, Lafayette, IN 47905

Jim Barlow

115. Ceradyne, Incorporated, 3169 Redhill Avenue, Costa Mesa, CA 92626
Joel P. Moskowitz

116–118. Ceramatec, Incorporated, 2425 South 900 West, Salt Lake City, UT 84119
Raymond Cutler
Ronald S. Gordon
David W. Richerson

119. Champion International Corporation, W. Nyack Road, W. Nyack, NY 10994
Dave Bennett

120. Cincinnati Milacron, 4165 Halfacre Road, Batavia, OH 45103-3247
Dean Reber

121. Colorado School of Mines, 1500 Illinois Street, Golden, CO 80410
George Krauss

122. Columbia Falls Alumina Co., 2000 Aluminum Dr., Columbia Falls, MT 59912
David Wilkening

123. Coors Glass - RMBC, 10619 W. 50th Ave., Wheatridge, CO 80033
Maurice Hanavan

124. Corhart Refractories, 1600 West Lee Street, Louisville, KY 40210
Michael Nelson

125–126. Corning Corporation, Sullivan Park FR-02-5, Corning, NY 14831
Thomas P. DeAngelis
Frank E. Murphy, Jr.

127. Corning Inc., Sullivan Park FR-2, Corning, NY 14831
F. Quan

128. Corning Incorporated, HP ME-2 E-5, Corning, NY 14830
John Wosinski

129–131. Cummins Engine Company, Incorporated, Mail Code 50183, P.O. Box 3005, Columbus, IN 47202-3005
Paul C. Becker
Magan J. Patel
James W. Patten

132. Dartmouth College, Thayer School of Engineering, Tuck Drive, Hanover, NH 03755
Ian Baker

133–134. DELPHI Saginaw Steering Systems, 3900 Holland Road, Saginaw, MI 48601-9494
Madhu Chatterjee
David M. Hitz

135. Delta M Corporation, 525 Warehouse Road, Oak Ridge, TN 37830
Reginald W. McCulloch

136. Doehler-Jarvis Technologies, Inc., P.O. Box 902, Toledo, OH 43691
H. Brucher

137–138. Dow Chemical Company, Inc., 1776 Building, Midland, MI 48674
David A. Dalman
Richard D. Varjian

139. Dow Chemical Company, 2301 N. Brazosport Blvd. B-251, Freeport, TX 77541-3257
Chris Kneupper

140. Dow Corning Corp., 4770 Highway 42 East, Carrollton, KY 41008
Charles A. Hall

141. DSF Refractories & Minerals Ltd., Friden, Newhaven, NR Buxton, Derbyshire SK17 0DX, England, U.K.
Paul Hutchinson

142. DuPont Central Research and Development, Experimental Station, Mail Stop E323/158, Route 141, P.O. Box 80323,Wilmington, DE 19880-0323
J. J. Barnes

143. DuPont Lanxide Composites Inc., 1300 Marrows Road, Newark, DE 19714-6077
Craig Shumaker

144–145. Duraloy Technologies, Inc., 120 Bridge Street, Scottsdale, PA 15683-1748
Roman Pankiw
Alan Paris

146. Dynamet Technology, Incorporated, 8 "A" Street, Burlington, MA 01803
Walter Bergler

147. Edison Welding Institute, 1250 Arthur E. Adams Drive, Columbus, OH 43210

Z. Feng

148–149. Electric Power Research Institute, Nuclear Plant Corrosion Control, 3412 Hillview Avenue, Palo Alto, CA 94303

Ben Banerjee
Mohamad M. Behravesh

150. Energetics, Incorporated, 7164 Gateway Drive, Columbia, MD 21046

Jack Eisenhower

151. EXXON R&D Labs, P.O. Box 2226, Baton Rouge, LA 70821

R. C. Schucker

152–155. A Finkl and Sons Co., 2011 Southport Ave., Chicago, IL 60614-4079

Guy Brada
Bruce C. Liimatainen
Carl Manthe
Algirdas Underys

156–158 FM Technologies, Incorporated, Patriot Square, 10529-B Braddock Road, Fairfax, VA 22032

P. Columbo
Gene A. Danko
Richard S. Silberglitt

159. FMC Corporation, Corporate Technology Center, Box 580, 1205 Coleman Avenue, Santa Clara, CA 95052

Michael T. Orillion

160. FMC Corporation, Corporate Technology Center, P.O. Box 8, Princeton, NJ 08543

Tony Nemzer

161–164. Ford Motor Company, P.O. Box 2053, Dearborn, MI 48121-2053

John E. Allison, Mail Drop 3182
William E. Dowling, Jr., MD3135/SRL
Kenneth Hass, Room S3028
Glen Weber

165. Forging Industry Association, 25 Prospect Avenue West, Suite 300, Cleveland, OH 44115

George Mochnal

166. Foster Wheeler Development Corporation, 12 Peach Tree Hill Road, Livingston, NJ 07039

Jeffrey L. Blough

167. General Electric Company, Research & Development, Met Building, Room 263, P.O. Box 8, Schenectady, NY 12301

Alan I. Taub

168. General Motors Corporation, 1660 L Street N.W., Suite 400, Washington, DC 20036

Bo Campbell

169–172. General Motors Corporation, AC Rochester, 1300 North Dort Highway, Flint, MI 48556

R. F. Beckmeyer
Lawrence A. Carol
W. LaBarge
Carl E. Miller

173. General Motors Corporation, 30500 Mound Road, Warren, MI 48090-9055

M. S. Rashid

174–178. General Motors Corporation, Saginaw Division, 3900 Holland Road, Saginaw, MI 48601-9494

Steven L. Avery
Randy P. Bal
Madhu S. Chatterjee
James Fargo
David H. Hitz

179. General Motors Powertrain Division, 895 Joslyn Road, Pontiac, MI 48340-2920

Ramesh Shah

180–181. George Mason University, 4400 University Drive, Fairfax, VA 22030

W. M. Black
R. F. Cozzens

182–185. Georgia Institute of Technology, School of Materials Engineering, 778 Atlantic Drive, Atlanta, GA 30332-0245

Steve Antolovich
W. Brent Carter
Joe K. Cochran, Jr.
Thomas L. Starr

186. Georgia-Pacific Corp., 133 Peachtree Street, N.E., 11th Floor, Atlanta, GA 30303

Karl T. Morency

187. Glass Industry Consulting, P.O. Box 6730, Lagons Miguel, CA 92607-6730

C. Philip Ross

188. Golden Technologies Company, Incorporated, Research & Development, 17750 West 32nd Avenue, Golden, CO 80401

Rick Kleiner

189–190. Harbison-Walker Refractories Company, 600 Grant St., Pittsburgh, PA 15219

Peter Antimarino
David V. Stiles

191. Hoskins Manufacturing Company, 10776 Hall Road, Hamburg, MI 48139

Forrest Hall

192–194. Idaho National Engineering Laboratory, EG&G Idaho, P.O. Box 1625, Idaho Falls, ID 83415-2218

Elmer Fleischman
D. Kunerth
E. S. Peterson

195–198. INCO Alloys International, P.O. Box 1958, 3200 Riverside Drive, Huntington, WV 25705-1771

Brian A. Baker
Pasupathy Gancsan
Vernon Hartmann
Gaylord D. Smith

199–201. Institute of Paper Science & Technology, Inc., 500 10th Street, N.W., Atlanta, GA 30318

David Orloff
Cheryl Rueckert
Preet Singh

202. International Paper, 6283 Tri-Ridge Boulevard, Loveland, OH 45140-7910

Subhash Pati

203–204. J&L Specialty Steel, Inc, One PPG Place, P.O. Box 3373, Pittsburgh, PA 15230-3373

Donald Hadfield
Paul Grandy

205. Jaakko Poyry Fluor Daniel, 100 Fluor Daniel Drive, Greenville, SC 29607-2762

Bo Oscarsson

206. James River Corporation, 1915 Marathon Avenue, P.O. Box 899, Neenah, WI 54957-0899

Bill Steed

207. James River Corporation, P.O. Box 2218, Richmond, VA 23217

Ronald Estridge

208. Jeffrey Chain Corporation, 2307 Maden Dr., Morristown, TN 37813-2898

David L. King

209. John Hopkins University, Center for Nondestructive Evaluation, Maryland Hall 107, Baltimore, MD 21218

Robert E. Green, Jr.

210. Johns Manville, P.O. Box 625005, Littleton, CO 80162-5005

Walter A. Johnson

211. Knauf Fiber Glass GmbH, 240 Elizabeth St., Shelbyville, IN 46176

Mike Carroll

212. KomTek, 40 Rockdale Street, Worcester, MA 01606

Michael Maguire

213–218. Kvaerner Pulping, 8008 Corporate Center Drive, Charlotte, NC 28226

Joe Barsin
Markku Isoniemi
Steve Koviack
Jussi Mantyniemi
Pertti Petane
Eric L. Wasson

219. Lawrence Berkeley National Laboratory, 1 Cyclotron Road, MS-62-203, Berkeley, CA 94720

Joel Ager

220–221. Lawrence Livermore National Laboratory, P.O. Box 808, Livermore, CA 94550

M. Fluss, Mail Stop L-326
Jeffery Wadsworth, Mail Stop L-353

222. Libbey Inc., P.O. Box 919, Toledo, OH 43616

James McGaughey

223–243. Los Alamos National Laboratory, P.O. Box 1663, Los Alamos, NM 87545

T. Archuleta, E549
R. S. Barbero, E549
A. H. Bartlett, G770
D. P. Butt, G755
D. W. Carroll, E549
R. G. Castro, G770
D. J. Devlin, E549
S. Gottesfeld, D429
K. J. Hollis, G770
W. R. Howell, Jr., J586
J. D. Katz, G771
H. H. Kung, G755
M. A. Miller, C331
M. A. Nastasi, K765
Y. Park, G755
J. J. Petrovic, G771
K. V. Salazar, E549
M. E. Smith, E549
M. Trkula, E549
G. J. Vogt, G771
K. C. Walter, K762

244. LTV Steel Company, Technology Center, 6801 Brecksville Road, Independence, OH 44131

F. J. Barchfeld

245. MacMillan Bloedel Packaging, Inc., Hwy 10, P.O. Box 336, Pine Hill, AL 36769

Wallace Baxter

246. Massachusetts Institute of Technology, Rm. 35-229, 77 Massachusetts Avenue, Cambridge, MA 02139-4307

Jung-Hoon Chun

247–248. National Institute of Standards and Technology (NIST), Gaithersburg, MD 20899

Edwin R. Fuller, Jr., Bldg. 223, Rm. A256,
Richard E. Ricker, Materials Bldg., Rm. B254

249. National Refractories & Minerals, 41738 Esterly Drive, P.O. Box 47, Columbiana, OH 44408-0047

Jim Houp

250–255. National Renewable Energy Laboratory, 1617 Cole Boulevard, Golden, CO 80401

Helena L. Chum, MS-1613
Satyen Deb, MS-3221
Robert J. Evans, MS-3311
Gregory Glatzmaier, MS-1613
Neil Kelley, MS3811
Stephen S. Kelley, MS-3311

256. Naval Research Laboratory, Bldg. 43, Rm. 212, Code 6000, 4555 Overlook Avenue, SW, Washington, DC 20735-5341

Bhakta B. Rath

257. National Science Foundation, Division of Material Research, 4201 Wilson Blvd., Arlington, VA 22230

Liselotte J. Shioler

258. Nooter Corporation, P.O. Box 451, St. Louis, MO 63166

Maan H. Jawad

259. North American Refractories, 3127 Research Dr., State College, PA 16801

Robert Antram

260. Northeastern University, 334 Snell Engineering Center, Boston, MA 02115

Teiichi Ando

261. Oregon State University, Oregon Street, Rog 414 OSU, Corvallis, OR 97331

Michael Kassner

262. Osram Sylvania Inc., 71 Cherry Hill Dr., Beverly, MA 01915-1068

William Rhodes

263. Osram Sylvania Inc., 1000 Tyrone Park, Versailles, KY 40383
Tom Hoffman

264–266. Owens Corning Corporation, Rt 16, 2790 Columbus Road, Granville, OH 43023-1200
Manoj Choudhary
Christopher Jian
John Petreanu

267. Parsons and Whittemore, Inc., Monroeville Office, P.O. Box 65, Perdue Hill, AL 36470
Adam Melton

268. Philip Morris, P.O. Box 26583, Richmond, VA 23261-6583
Mohammad R. Hajaligol

269–270. Philip Morris U.S.A., P.O. Box 26603, Richmond, VA 23261
John Dawson
Richard Webb

271–272. Polymet Corporation, 10073 Commerce Park Drive, Cincinnati, OH 45246
William C. Mosier
Steve Zorko

273–274. Potlatch Corporation, Lewiston, ID 83501-1016
Larry Butts
Gerald Cran

275. Powdermet, 416 Trinity Court, Petaluma, CA 94954
Animesh Bose

276–279. PPG Industries, Inc., Glass Technology Center, P.O. Box 11472, Harmarville, PA 15238-0472
Warren Curtis
Ganjiang Feng
Amar Mishra
George Pecoraro

280. Process Simulations Ltd., (CFD consultant for Weyerhauser), Box 1125, Station A, Delta, B.C. V4M 3T2
Zia Abdullah

281–282. Pulp and Paper Research Institute of Canada, Vancouver Laboratory, 3800 Westbrook Mall, Vancouver, B.C. V6S 2L9

Robert Prescott
Douglas Singbeil

283. Queen City Forging Company, 235 Tennyson Street, Cincinnati, OH 45226

Rob Mayer

284–285. Rapid Technologies, Incorporated, P.O. Box 368, 170 Werz. Ind. Blvd., Newnan, GA 30264

Ed Dailey
Andrew Tomys

286. Rensselaer Polytechnic Institute, School of Engineering, Materials Engineering Department, 8th Street, Troy, NY 12180-3590

N. S. Stoloff

287. Rouge Steel Company, 3001 Miller Rd., P.O. Box 1699, Dearborne, MI 48121-1699

Dennis Crosby

288–294. Sandia National Laboratories, 7011 East Avenue, P.O. Box 969, Livermore, CA 94551-0969

M. D. Allendorf, MS-9052
S. M. Ferko, MS-9052
S. Griffiths, MS-9042
D. R. Hardesty, MS-9052
A. H. McDaniel, MS-9052
R. Nilson, MS-9042
G. A. Samara, MS-1421

295. Sandia National Laboratories, University of New Mexico, Advanced Materials Laboratory 1708, 1001 University Boulevard, SE, Suite 100, Albuquerque, NM 87106

W. G. Fahrenholtz

296–303. Sandia National Laboratories, 1515 Eubank, S.E., P.O. Box 5800, Albuquerque, NM 87185-5800

C. J. Brinker, Mail Stop 1349
Bob Eagan, Mail Stop 0513
K. G. Ewsuk, Mail Stop 1349
J. B. Kelley, Mail Stop 1134
R. E. Loehman, Mail Stop 1349
P. I. Pohl, Mail Stop 0720
R. D. Skocypec, Mail Stop 0835
A. P. Sylwester, Mail Stop 0710

304–308. Sandusky International, 615 W. Market Street, P.O. Box 5012, Sandusky, OH 44871-5012

Steve Furey
Greg Michel
John Rogers
Edward Ryan
Dan Scott

309–310. Sandvik Steel Co., P.O. Box 1220, Scranton, PA 18501-1220

Gary Boberick
Jim Noble

311. Schuller International, Inc., P.O. Box 517, Toledo, OH 43697-0517

Don Shamp

312. Siebe Automotive, P.O. Box 400, Knoxville, TN 37919

Manny Tuli

313. Shenango Industries, Inc., P.O. Box 2069, Terre Haute, IN 47802

Ian Sadler

314–316. Southern Illinois University, Dept. of Mechanical Eng. and Energy Process, Carbondale, IL 62999

Rasit Koc
C. Meng
G. A. Swift

317. St. George Crystal, Brown Ave., P.O. Box 709, Jeannette, PA 15644

Jerry Kynik

318. Stoody Company, 5557 Nashville Road, Bowling Green, KY 42101-7546

Ravi Menon

319. Techneglas, 727 E. Jenkins Ave., Columbus, OH 43207
Jim Shell

320. Thermo Electron Technologies, 85 First Avenue, Waltham, MA 02254
Peter Reagan

321–322. The Timken Company, 1835 Dueber Avenue, S.W., Canton, OH 44706-2798
Robert L. Leibensperger
Jeffrey C. Moscsari

323. The Timken Company, P.O. Box 6930, Canton, OH 44706-0930
Katherine Hylton

324. The Timken Company, P.O. Box 6932, GNW-19, Canton, OH 44706-0932
Erich D. Dominik

325. Trinity Forge, 947 Trinity Drive, Mansfield, TX 76063
Muhammed Abbas

326. Truecast, 6761 Cane Run Rd., P.O. Box 58610, Louisville, KY 40258
David Hubbard

327. TRW, Incorporated, 23555 Euclid Avenue, Cleveland, OH 44117
A. L. Bement, Jr.

328–329. U.S. Air Force, Wright Patterson AFB, Dayton, OH 45433-6533
Dennis M. Dimiduk, WRDC Material Laboratory
Allan Katz, AFWAL/MLLM Material Laboratory

330–358. U.S. Department of Energy, 1000 Independence Avenue, SW, Washington, DC 20585

Rolf F. Butters, EE-24
Joseph Carpenter, EE-32
H. Bruce Cranford, EE-21
Sidney Diamond, EE-34
Sara Dillich, EE-22
Thomas D. Foust, EE-21
Deborah A. Haught, EE-23
Marvin E. Gunn, Jr., EE-60
M. Patricia Hoffman, EE-23
Ramesh Jain, EE-22
Gobind Jagtiani, EE-22
Theodore Johnson, EE-21
Douglas E. Kaempf, EE-22
William P. Parks, Jr., EE-23
Marsha L. Quinn, EE-24
Scott L. Richlen, EE-21
Valri Robinson, EE-21
Peter H. Salmon-Cox, EE-20
Robert B. Schulz, EE-34
Kurt Sisson, EE-21
Merrill A. Smith, EE-21
Charles A. Sorrell, EE-23
Louis Sousa, EE-20
Denise F. Swink, EE-20
Brian G. Volintine, EE-22
Ingrid Watson
Daniel E. Wiley, EE-21
Stanley M. Wolf, EM-54
Harvey Wong, EE-21

359–362. U.S. Department of Energy, 19901 Germantown Road, Germantown, MD 20585

Fred Glaser, FE-72
Robert J. Gottschall, ER-13
Helen Kerch, ER-13
F. W. Wiffen, ER-52

363. U.S. Department of Energy/Albuquerque, P.O. Box 5400, Albuquerque, NM 87115

D. Morton

364. U.S. Department of Energy/Oak Ridge, P.O. Box 2008, Oak Ridge, TN 37831-6269

Mary Rawlins

365. U.S. Department of Energy/Idaho, 785 Dow Place, Idaho Falls, ID 83402

Joanne Malmo

366. Union Camp Corporation, P.O. Box 3301, Princeton, NJ 08543-3301

Dave Crowe

367–370. United Defense, Steel Products Div., 2101 West 10th St., Box 1030, Anniston, AL 36202

John Boggan
Elmer L. Doty
Gary E. Hudson
Nectar L. Ramirez

371. United Technologies Pratt & Whitney, 1700 Beeline Highway, Jupiter, FL 33478

Donald R. Clemens

372–374. Universal Energy Systems, Inc., 4401 Dayton-Xenia Road, Dayton, OH 45432-1894

Hal Gagel
Young-Won Kim
Mark Sammons

375. University of Alabama, Metal Casting Technology Center, P.O. Box 6374, Tuscaloosa, AL 35487

Thomas S. Piwonka

376. University of Idaho, Institute for Materials and Advanced Processes, Mines Building, Room 321, Moscow, ID 83844-3026

F. H. Froes

377. University of Maine, 5737 Jenness Hall, Orono, ME 04469-5737

Marquita Hill

378. University of Missouri at Rolla, 224 McNutt Hall, Rolla, MO 65401

Robert E. Moore

379–380. University of Tennessee, Dept. of Materials Science & Engineering, Knoxville, TN 37996-2200

C. R. Brooks
Ben F. Oliver

381. Vander Linden & Associates, 5 Brassie Way, Littleton, CO 80123
Carl R. Vander Linden

382. Virginia Polytechnic Institute and State University, 231 Holden Hall, Blacksburg, VA 24061
S. B. Desu

383. Virginia Polytechnic Institute and State University, 213 Holden Hall, Blacksburg, VA 24061-0237
B. J. Love

384. Visteon Glass System, 15000 Commerce Drive, North, Dearborn, MI 48120
Vincent Henry

385. Weirton Steel Corporation, 400 Three Springs Drive, Weirton, WV 26062
James J. Brinsky

386. Weirton Steel Corporation, 500 Three Springs Drive, Weirton, WV 26062
Robert Hammerton

387. Welding Services, Incorporated, 2110 Pebble Beach Drive, Suite 100, Carmel, IN 46032
George Lai

388–389. Welding Services, Incorporated, 2225 Skyland Court, Norcross, GA 30071
Mike Jirinec
David A. Joiner

390. Wescast Industries, Inc., P.O. Box 1930, 799 Powerline Road, Brantford, ON N3T 5W5, Canada
Richard W. Williams

391. West Virginia University, Mechanical and Aerospace Eng. Dept., P.O. Box 6106, Morgantown, WV 26506-6106
Larry Banta

392–393. West Virginia University, P.O. Box 6064, Morgantown, WV 26506-6064
Keh-Minn Chang
Carl Irwin

394–395. Westinghouse Electric, 4400 Alafaya Trail, Orlando, FL 32826
Steve Breitenbach
Mahmood Choudry

396–399. Westvaco, Laurel Technical Center, 11101 Johns Hopkins Road, Laurel, MD 20723-6006

Abbie Alavi
Lad Falat
Greg Makar
Sandy Sharp

400. Weyerhaeuser Paper Company, Columbus Pulp and Paper Complex, P.O. Box 1830, Columbus, MS 39703-1830

Joe May

401–407. Weyerhaeuser Paper Company, Research and Development, WTC 2H22, Tacoma, WA 98477

Dick Ericson
Jules V. Gommi
Margaret Gorog
Peter Gorog
Denny Hunter
Del Raymond
Dick Shenk

408. Worcester Polytechnic Institute, Department of Mechanical Engineering, 100 Institute RJ, Worcester, MA 01609

Robert N. Katz

409. Wyman-Gordon Forging, 10825 Telge Road, Houston, TX 77095-5038

Ronald A. Wallis

410. Wyman-Gordon Company, 244 Worcester Street, P.O. Box 8001, North Grafton, MA 01536-8001

Sanjay N. Shah

411. X Form, Inc., 100 North Mohawk Street, Box A-9, Cohoes, NY 12047

Karl Shaw

412. 127 West View Lanes, Oak Ridge, TN 37830

James Wessell

413. 225 Linden Court, Sewickley, PA 15143

William E. Dennis

414. 3M Industrial & Electronic Sector, Research Laboratory, Building 201-4N-01, 3M Center, St. Paul, MN 55144-1000

Ross H. Plovnick